frontiers | Frontiers in Energy Research

ORIGINAL RESEARCH
published: 22 July 2022
doi: 10.3389/fenrg.2022.830845

Biodiesel Synthesis From *Cucumis melo* Var. *agrestis* Seed Oil: Toward Non-food Biomass Biorefineries

Maria Ameen[1], *Muhammad Zafar*[1], *Abdul-Sattar Nizami*[2,3]*, *Mushtaq Ahmad*[1], *Mamoona Munir*[1,4], *Shazia Sultana*[1], *Anwar Usma*[1] *and Mohammad Rehan*[3]

[1]Biofuel Laboratory, Department of Plant Sciences, Quaid-i-Azam University, Islamabad, Pakistan, [2]Sustainable Development Study Center, Government College University, Lahore, Pakistan, [3]Centre of Excellence in Environmental Studies (CEES), King Abdulaziz University, Jeddah, Saudi Arabia, [4]Department of Botany, Rawalpindi Women University, Rawalpindi, Pakistan

This study aims to examine the potential of non-edible seed oil (*Cucumis melo* var. *agrestis*), seed oil content 29.1%, FFA 0.64 (mg KOH/g) for biodiesel production via nano-catalyst. The catalyst was characterized using X-ray diffraction spectroscopy (XRD), Fourier transform infrared spectroscopy (FTIR), scanning electron microscopy (SEM), and energy dispersive X-ray spectroscopy (EDX). The maximum biodiesel yield (93%) was attained under optimized conditions, i.e., 9:1 methanol to oil molar ratio, 2 wt% catalyst (MgO) at 60°C. The synthesized biodiesel yield was optimized through response surface technology via Box Behnken design (BBD). Biodiesel was characterized by advanced analytical techniques, including gas chromatography and mass spectroscopy, FTIR, and nuclear magnetic resonance (NMR). Fuel properties of synthesized biodiesel, including density (0.800 kg/L), K. viscosity @ 40°C (4.23 cSt), cloud point −12°C, pour point −7°C, sulfur content (0.0001%), flash point (73.5°C), total acid no (0.167 mg KOH/g) were found in lines with international standard of American Society of Testing Materials (ASTM). *Cucumis melo* var. *agrestic* seed oil and nano MgO catalyst appeared as economical, sustainable, and feasible candidates to overcome global energy glitches and environmental issues. The study findings involving unpalatable seed oil will be a promising step toward non-food biomass biorefinery.

Keywords: Cucumis melo var. agrestris, nano-catalyst, transesterification, biorefinery, fuel characterization

OPEN ACCESS

Edited by:
Uwe Schröder,
University of Greifswald, Germany

Reviewed by:
Balajii Muthusamy,
PSG College of Technology, India
Muhammad Farooq,
University of Engineering and Technology, Pakistan

***Correspondence:**
Abdul-Sattar Nizami
nizami_pk@yahoo.com

Specialty section:
This article was submitted to Bioenergy and Biofuels, a section of the journal Frontiers in Energy Research

Received: *07 December 2021*
Accepted: *02 June 2022*
Published: *22 July 2022*

Citation:
Ameen M, Zafar M, Nizami A-S, Ahmad M, Munir M, Sultana S, Usma A and Rehan M (2022) Biodiesel Synthesis From Cucumis melo Var. agrestis Seed Oil: Toward Non-food Biomass Biorefineries. Front. Energy Res. 10:830845. doi: 10.3389/fenrg.2022.830845

1 INTRODUCTION

Due to economic development, energy demand has increased with time. Overpopulation, urbanization, and deforestation have laid the foundation for this energy gap (Mahlia et al., 2020). Moreover, it has deteriorated the ecosystem by creating severe environmental concerns such as intensifying local air pollution, ozone depletion, acid rain, and global warming (Rahman et al., 2017). It is due to the emission of hazardous gases like CO_2, SO_x, NO_x, CO, and hydrocarbons produced during fossil fuel combustion that cause the greenhouse effect (Ahmad et al., 2011a; 2013; Mumtaz et al., 2021). The primary source for fulfilling basic energy needs is regular non-renewable petroleum-based fuel (Ullah et al., 2018). Finite deposits of conventional fuel are squeezing and exhausting fast due to continuous indiscriminate consumption and overexploitation (Cheema et al., 2021). This hasty decline of natural fuel reserves and linked petroleum price hikes have searched for alternative energy sources indispensable and accelerated their exploration and utilization (Dai et al.,

2015). The only way forward and a conniving strategy to minimize greenhouse gas emissions and overcome fuel scarcity is to develop a renewable alternate that may resolve such disconcerting ecological alarms (Sharma et al., 2020). Like other renewable sources such as solar energy, hydropower, wind energy, and geothermal energy, biofuels have also shown promising results in satisfying energy demands and assisting in the impact alleviation of abrupt climate change (Antero et al., 2020; Li et al., 2020).

Biofuels such as biogas, bioalcohols, bioether, and biodiesel have attracted great attention as promising stand-ins for traditional fossil fuels because of human health hazards and climate change over the past 25 years (Ahmad et al., 2011b; Callegari et al., 2020). Among these options, biodiesel has emerged as a promising replacement for petrodiesel because its consumption is linked with nitrogen oxide emission, which grasps greenhouse gases in extra amounts (Wang et al., 2021; Yusuff et al., 2021). Pre-combustion and post-combustion techniques can be altered to reduce nitrogen oxides (Ahmad et al., 2011c). Fatty acids in long chains forming monoalkyl esters are termed biodiesel. It has been acknowledged as an attractive solution for diminishing finite petroleum-based diesel fuel over the past few decades. A remarkable reason for selecting biodiesel as a potential fossil fuel substitute is its equivalent properties and analogous property to petroleum diesel (Ahmad et al., 2015; Babu et al., 2020; Razzaq et al., 2020a). Biodiesel is an ecological, harmless, clean-burning fuel free of aromatics and sulfur content. Biodiesel is considered a prominent natural, economically competitive, eco-friendly, and technically viable, and its usability and high combustion efficiency in the same engine with little or no mechanical modifications (Khan et al., 2020). It endeavors additional supremacies over regular diesel, including non-toxicity, sustainability, and biodegradability. Other attributes of diesel with biological origin include high flash point, super-lubricity, less viscosity, better cetane number, and equitable cold filter plugging point. These primacies make it an encouraging liquid reserve for regular fuel (Khan et al., 2021; Saeed et al., 2021).

Biodiesel is derived from various sources: microalgae, animal fat, vegetable oil, algae, oils from the fungal origin, terpenes, latex, edible waste oil, or surplus cooking oil from household and commercial practices (Ahmad et al., 2011d; Saeed et al., 2021). Animal fats include poultry, beef tallow, fish, and pork lard. For many years, edible vegetable oils such as sorghum, sunflower, barley, peanut, oat, and coconut have been used. About 17% of total grain produced globally is used to produce biodiesel. However, due to their competition with food supply-demand, non-edible vegetable oils are preferable feedstock for biofuel synthesis (Rehan et al., 2018; Gardy et al., 2019). Biodiesel feedstock must satisfy two provisions: low production cost and a large production scale. Non-edible oil-yielding seed plants, including *Raphanus sativus* (Cavalheiro et al., 2021), *Raphanus raphanistrum* (Munir et al., 2021a), *Prunus cerasoids* (Munir et al., 2019a), and *Lepidium perfoliatum* (Munir et al., 2019b) have the potential to act as cheap feedstock. These sources play an ideal role in dealing with food insecurity. Indigenous non-edible feedstock has been figured out as significant recompense to mitigate air pollutants and probably shun the food supply controversy debate.

Cucumis melo var. *agrestis,* small gourd or musk melon, is an annual or perennial herbaceous climbing vine that belongs to the family Cucurbitaceae and is found all over the old-world tropics (Sahithi et al., 2015). The stem is covered with scabrous hair, prostrate but branched. Leaves are scabrid, have rigid hair, 3–5 (-7) lobed, and 1–6 cm long petiole. Flowers are solitary, small, sometimes in pairs or threes with 5–10 mm long peduncles. The flowering season is June, July, and August. Fruit is smooth, glabrescent, round, oval-globose, and ellipsoid, usually with dark green stripes. Fruit size is about 2.5–5 cm in diameter. Wild musk melon grows abundantly in wild rice fields, trash, vacant lots, unoccupied houses, roadsides, rail tracks, meridians, and disturbed places (Nesom, 2011). The fruit of wild muskmelon is also cooked as a vegetable, but seeds are discarded as non-edible because sprouting seeds contain toxic substances in the embryo. However, its seeds also contain a substantial quantity of oil (29.1%), just like other melons (30% oil approx.), as shown in **Supplementary Figure S1**. Hence, *Cucumis melo* var. *agrestis* can be a non-edible and promising candidate for biodiesel production (Ameen et al., 2018). In 2007, the annual production of *Cucumis melo* L. was recorded as >26 million tons, cultivated as a vegetable crop representing a significant seed production (Nuñez-Palenius et al., 2011). Asia, with 74% (31,166,896 tons) of world production, is considered the largest producer of melons, followed by America and Europe with 11.9 and 7.2% production, according to FAOSTAT data from 2008 to 2016 (FAOSTAT 2017a) and a decrease in melon production in Europe (2,274,736 tons to 739,289 tons). If 30% oil content is considered on average, then 52,179 tons of seed oil can be produced (Silva et al., 2020). According to FAO, i.e., the food and agriculture organization, 782,205 tons of melon seeds are produced across the globe (Food and Agriculture Organization of the United Nations, 2013; Petkova & Antova, 2015; FAOSTAT 2017b). The approximate global production of melon crops stated by Napolitano et al., 2020 was 31.9 M tons in 1.2 M hector harvested area. Asia produces 24.1 M tons, Europe 1.8 M tons, and America 3.6 M tons (Napolitano et al., 2020; Ameen et al., 2021).

Biodiesel or fatty acids methyl esters (FAMEs) are produced via transesterification of fats and oils (triglycerides) using methanol in the presence of suitable catalysts like homogeneous catalysts such as acids and bases (H_2SO_4, HCl, KOH, and NaOH), heterogeneous catalyst such as bases (Alkali metals, and Alkaline earth metal-based catalyst, mixed metal-based, transition metal-based, Hydrotalcite-based, waste-based catalysts), and acids (Cation exchange resins, heteropolyacid derivatives, sulfated oxide based and sulphonic acid-based catalysts), Acid/Base catalyst (Zirconia, and zeolite-based) (Munir et al., 2021b), biocatalysts like enzymes, nano-catalysts ($CaO/CuFe_2O_4$, $MgO/MgAl_2O_4$, and $Cs/Al/Fe_3O_4$) (Ahmad et al., 2015; Oueda et al., 2017; Thangaraj et al., 2019). In general, biodiesel is produced at the industrial level via homogeneous catalysts. However, such catalysts offer higher yields yet are coupled with several demerits (difficulty of neutralization, excessive methanol requirement, washing and drying for

removal of glycerol and catalyst leading to wastage of water and rise in product cost) (Yang et al., 2014). In contrast, green heterogeneous catalysts are attaining considerable attention for their potential competency in overcoming the shortcomings of homogeneous catalysts in biodiesel synthesis (Pasae et al., 2020). Heterogeneous nano-catalysts have gained popularity among researchers for the efficient conversion of oils to biodiesel owing to their high conversion rate, catalytic efficiency, good rigidity, large surface area, and great resistance to saponification (Gardy et al., 2017, 2018). Nanoparticles are pseudo-spherical and <100 nm in diameter, involved in enhancing reaction rate by lowering the activation energy of reactants so that they can be readily converted into products. Various nano-catalysts have been experienced to synthesize biodiesel, such as $K_2O/c\text{-}Al_2O_3$ $KF/C\text{-}Al_2O_3$, Fe_3O_4 amorphous alumina, $Cs\text{-}Ca/SiO_2\text{-}TiO_2$, and potassium bitartrate with zirconia. In addition, nano-catalysts are recoverable, green, i.e., environment-friendly, non-corrosive, and no post-treatment washing is required (Bet-Moushoul et al., 2016; Dawood et al., 2018). Alkali-based catalysts offer relatively higher conversion efficiency than acid catalysts among heterogeneous solid catalysts. Because they have a large surface area (compared to bulky substances), stable rigor, pronounced confrontation to saponification, and high catalytic efficiency; hence, they are considered more active catalysts during transesterification reactions (Ingle et al., 2020; Li et al., 2020).

Previous studies revealed that solid base metal oxides give likely results, such as Fe_2O_3 MnO SO_4^{2-}/ZrO_2, showing a 96.5% biodiesel yield (Alhassan et al., 2015; Razzaq et al., 2020). The nano-sized MgO catalyst of 5.5 nm was used to transesterify goat fat, and a 93.12% yield was achieved (Rasouli & Esmaeili, 2019). Dawood and coworkers (2018) used MgO nanoparticles of 70–90 nm size to convert yellow oleander into respective methyl ester, and 93.1% biodiesel yield was achieved (Dawood et al., 2018). MgO nano-catalyst has been widely used on different feedstocks like yellow oleander, i.e., Silybum eburneum seed oil. For that, 91% biodiesel yield was obtained by applying MgO with the size of 13 nm (Shaheen et al., 2018). *Moringa oleifera* seed oil was converted to 93.69% under optimized conditions using the Taguchi method. (Esmaeili et al., 2019). MgO nano-catalyst has been used in the form of nanocomposites such as waste edible oil, has been converted into biodiesel by application of CaO@MgO as a catalyst and reused up to six cycles, and 98.37% biodiesel yield was achieved (Foroutan et al., 2020). The catalytic activity of nanocrystalline MgO catalysts in nanosheets on sunflower oil and rapeseed oil produces biodiesel (Verziu et al. (2008). High conversion yield via MgO nano-catalyst was achieved under microwave conditions as compared to autoclave or ultrasound due to high selectivity (Akia et al., 2014). Literature supports that a lot of work has been done on biodiesel production by MgO nano-catalyst. However, no research has been conducted yet on its catalysis in the transesterification of *Cucumis melo* var. *agrestis* seed oil. Although, biodiesel synthesized from *Cucumis melo* var. *agrestis* seed oil by using a homogeneous catalyst has been reported (Ameen et al., 2018). However, applying nano-sized MgO catalyst on non-edible seed oil of Cucumis melo var. agrestis is a novel study to the best of our knowledge. Therefore, the current study focused on producing biodiesel from *Cucumis melo* var. *agrestis* seed oil using MgO nano-catalyst. The as-synthesized nano-catalyst (MgO) was characterized by diverse analytical techniques such as X-ray diffraction (XRD), scanning electron microscopy (SEM), energy dispersive X-ray (EDX), and Fourier transform infrared spectroscopy (FTIR). The quality and fuel properties of the produced biodiesel were further determined using FTIR, GC-MS, ^{1}HNMR, and ^{13}CNMR. Fuel properties of synthesized biodiesel were further compared with international standards of American Society for Testing and Materials (ASTM).

2 MATERIALS AND METHODS

2.1 Reagents and Equipment

Seed collection was carried out from local wild fields in the vicinity of Tehsil Talagang of district Chakwal, Pakistan. The reagents used were isopropyl alcohol, phenolphthalein, petroleum ether (RCl Labscan 95% pure), potassium hydroxide (KOH), ethanol absolute (C_2H_5OH) scharlau 99.8% pure, sodium hydroxide (NaOH) scharlau extra pure, magnesium sulfate heptahydrate (Sigma Aldrich), and methanol (CH_3OH) Merck Germany with 99.9% purity, and chloroform (Scharlau extra—pure). Reagents and chemicals were used without any further purification as purchased.

2.2 Oil Extraction

Washed seeds were oven-dried (55°C) for the removal of moisture content. Determination of oil content in seeds was done chemically by solvent extraction technique using soxhlet apparatus (behr Labor-Technik). Petroleum ether (250 ml) was taken in a round bottom flask, and well-powdered seeds (15 g) of *Cucumis melo* var. *agrestis* were taken in a thimble. The whole process was carried out at a specific heating temperature (60°C) for 6 h, and seed oil droplets were collected in a round bottom flask. The following equation computed the oil yield of seeds.

$$\text{Oil yield } (\%) = \frac{\text{Weight of oil extracted}}{\text{Weight of sample used}} \times 100 \qquad (1)$$

However, mechanical oil extraction was carried out via an electric oil expeller, followed by crude oil collection in containers of the required size. Oil expulsion from seeds of the known amount was completed after three to five turns. The chemical oil extraction was carried out to determine oil contents in *Cucumis melo* var. *agrestis* seeds, and mechanical oil extraction was done to obtain oil in large quantities for this study's experimental work. Biodiesel feedstock and products are shown in **Supplementary Figure S2**.

2.3 Free Fatty Acid Content Determination

The aqueous acid-base titration method was used to investigate the FFA content (%) of *Cucumis melo* var. *agrestis* seed oil. In this protocol, blank and sample titrations were performed. By dripping 0.025 M KOH solution from the burette in a conical flask containing isopropanol (10 ml) and phenolphthalein (Solution) as an indicator. Whereas sample titration involves titration of oil (1 ml) and isopropanol (9 ml) and two to three drops of phenolphthalein in conical flask against KOH (0.025 M)

until the appearance of an endpoint (pink color). After three concordant readings, the following formula was applied to analyze the FFA content of crude oil (Munir et al., 2020)

$$\text{Acid number} = \frac{(A - B) \times C}{D} \quad (2)$$

A and B are volume of KOH used in sample and blank titration, whereas C is catalyst amount (g/L) and D is oil (vol.) used in sample titration (Munir et al., 2019a; Dawood et al., 2020).

2.4 Catalyst Synthesis

The coprecipitation method was adopted with minor modifications (Shahzad et al., 2017; Ashok, Kennedy, Vijaya, & Aruldoss, 2018). In the burette, 0.1 M (100 ml soln.) magnesium sulfate ($MgSO_4$) was taken and titrated against a continuously stirring solution (500 rpm) of 0.1 M sodium hydroxide (NaOH) in a conical flask until basic pH (10) was attained. Repeated washing of productive solution for purification was followed by oven drying at 90 ℃ for 12 h to eliminate moisture. The dried sample taken in a china dish was kept in a muffle furnace at 500 ℃ for 3 h resulting in the synthesis of fine amorphous nanoparticles. The sample was now ready for analysis (Shaheen et al., 2018). In order to achieve the highest possible catalytic activity, the calcination temperature of 500°C for 3 h was selected. Because the calcination temperature and duration time significantly affect the microstructure and reactivity of MgO. The size of MgO particles grows bigger at a higher temperature. Literature reports reveal the effects of calcination temperature and duration time on (SSA) of MgO that can be clearly seen as the specific surface area (SSA) decreases when the calcination temperature and duration time increase than optimum. Moreover, the catalyst has greater porosity at this temperature and a large surface area to form the active sites as compared to lower or higher temperature and time duration of more or less than 3 h; this optimum temperature and time duration correspond to high catalytic activity due to decrease in activation energy (Rashid et al., 2018; Rozina et al., 2019; Khan et al., 2021).

2.5 Characterization of Catalyst

The diffraction pattern of synthesized nano-catalyst (MgO) was analyzed by powder XRD (Bruker—Model# D8) in the range (2θ = 10°–60°), Cu-Kα (1.54 A°) with scan rate (2° in 2θ/min). Fourier transform infrared spectroscopic (FTIR) analysis of MgO nano-catalyst was done via PerkinElmer Spectrum 65 within the range of 515–4,000 cm^{-1} to identify chemical bonds and functional groups present in the molecule.

SEM images were taken via 20 KV accelerating voltage using field emission of the scanning electron microscope (JOEL JSM5910). Catalyst surface is qualitatively characterized by SEM and aid in the interpretation of phenomena that occurs during calcination and pretreatment of catalyst. The EDX technique was used to examine the chemical composition of MgO nano-catalyst. The EDX spectrum in the range of 0–1,350 eV was used to examine MgO nano-catalyst.

2.6 Reflux Transesterification of Oil to Biodiesel

Transesterification was carried out in a round bottom flask associated with a condenser for averting methanol escape and a magnetic stirrer. A known volume of filtered oil (100 ml) was preheated in a three-necked round bottom flask (250 ml) followed by catalyst addition dispersed in methanol since low FFA content 0.64 mgKOH/g within fixed limits favors single-step transesterification. In optimization reactions, the oil to methanol ratio (1:3 to 1:15), reaction time (1–6 h), and temperature (60–120 ℃), as well as catalyst amount (0.5–3.5% wt. of oil taken), were adjusted to an optimum level. On completion of the reaction, the mixture was centrifuged at 4,000 rpm for 5 min. Then, the mixture was transferred in a separate funnel to separate FAMEs (upper layer), catalyst, and glycerol (lower layer). Finally, the excess methanol was removed from the reaction mixture using a rotary evaporator. The biodiesel yield was estimated by the equation (Munir et al., 2019b):

$$\text{Biodiesel Yield } (\%) = \frac{\text{Biodiesel produced } (g)}{\text{Oil used } (g)} \times 100 \quad (3)$$

2.7 Biodiesel Characterization

FTIR spectra of biodiesel were developed on a Derkin Elmer, model spectrum 65 in the range of 400–4,000 cm^{-1}; 15 scans to analyze biodiesel and at 1 cm^{-1} resolution to get an insight into the functional groups as the presence of FAMEs and their structural arrangement. ^{1}HNMR (300 MHz) and ^{13}CNMR (75 MHz) spectroscopies involving 30°pulse duration, 1.0 s, and 8 scans, while 1.89 s and 160 scans recycle delays, respectively. Both were done using deuterated $CDCl_3$ as solvent via Avan CE 300 MHz spectrometers at 7.05 T.

Fuel properties of newly produced biodiesel of *Cucumis melo* var. *agrestis* seed oil were quantitatively determined and matched with ASTM D 6751 such as kinematic viscosity @40 ℃cSt ASTM D445, density @ ℃ Kg/L ASTM D-1298, total acid number (mg KOH/gm) ASTM D-974, sulfur content (% wt.) ASTM D-4294, pour point ASTM D-97, cloud point ASTM D-2500 and flashpoint ℃ (PMCC) ASTM D-93.

2.8 Experimental Scheme for Biodiesel Production

Response surface methodology (RSM) based on Box Behnken design (BBD) prepared using Design Expert 13, Stat-ease Inc., Minneapolis, United States, for investigation of the effect of different independent variables including methanol: oil (Met: Oil), amount of catalyst used, reaction time, and temperature required to complete a reaction. Thirty experiments were conducted for four factors having maximum and minimum ranges, i.e., 1) methanol to oil molar ratio taken within range, 3:1 to 15:1 2) reaction time 60–360 min 3) catalyst loading 0.5–3.5 wt% 4) reaction temperature 60–120℃. **Supplementary Table S1** represents the range and levels of independent parameters for the BBD.

TABLE 1 | Comprehensive experimental results of biodiesel synthesis reaction.

Run	A:Alcohol to Oil Molar Ratio	B:Reaction Time (min)	C: Catalyst Loading (wt%)	D:Temperature ◦C	Yield %
1	9:1	210	2	120	89
2	9:1	210	0.5	60	70
3	3:1	60	0.5	120	60
4	15:1	360	0.5	120	68
5	15:1	360	3.5	120	60
6	15:1	360	0.5	60	65
7	15:1	360	3.5	60	50
8	9:1	210	2	60	77
9	15:1	60	3.5	60	63
10	9:1	210	2	90	89
11	3:1	360	0.5	60	64
12	3:1	360	3.5	60	66
13	15:1	60	0.5	60	70
14	3:1	60	3.5	120	45
15	3:1	60	0.5	60	58
16	9:1	210	2	90	90
17	15.1	210	2	90	78
18	9:1	210	3.5	90	65
19	15:1	60	0.5	120	50
20	9:1	210	2	90	89
21	9:1	210	2	60	83
22	9:1	60	2	90	70
23	9:1	210	0.5	90	65
24	3:1	60	3.5	60	42
25	3:1	360	0.5	120	40
26	9:1	360	2	90	93
27	3:1	360	3.5	120	50
28	9:1	210	0.5	90	60
29	3:1	210	2	90	55
30	15:1	60	3.5	120	50

TABLE 2 | Analysis of variance (ANOVA) for RSM.

Source	Sum of Squares	df	Mean Square	F-value	*p*-value	—
Model	5049.59	14	360.69	3.67	0.0087	significant
A-Alcohol to oil molar ratio	304.22	1	304.22	3.10	0.0988	—
B-Reaction time	128.00	1	128.00	1.30	0.2715	—
C-Catalyst loading	97.40	1	97.40	0.9918	0.3351	—
D-Temperature	85.47	1	85.47	0.8703	0.3657	—
AB	1.56	1	1.56	0.0159	0.0013	—
AC	7.56	1	7.56	0.0770	0.7852	—
AD	14.06	1	14.06	0.1432	0.0104	—
BC	45.56	1	45.56	0.4639	0.5062	—
BD	0.0625	1	0.0625	0.0006	0.0802	—
CD	29.70	1	29.70	0.3024	0.5905	—
A^2	467.73	1	467.73	4.76	0.0454	—
B^2	18.00	1	18.00	0.1833	0.6747	—
C^2	1225.55	1	1225.55	12.48	0.0030	—
D^2	8.32	1	8.32	0.0847	0.7751	—
Residual	1473.21	15	98.21	—	—	—
Lack of Fit	1442.04	11	131.09	16.83	0.0075	significant
Pure Error	31.17	4	7.79	—	—	—
Cor Total	6522.80	29		—	—	—
R^2 0.7741, Std. Dev 9.91, C.V. % 15.06, Adeq. Precision 6.2860						

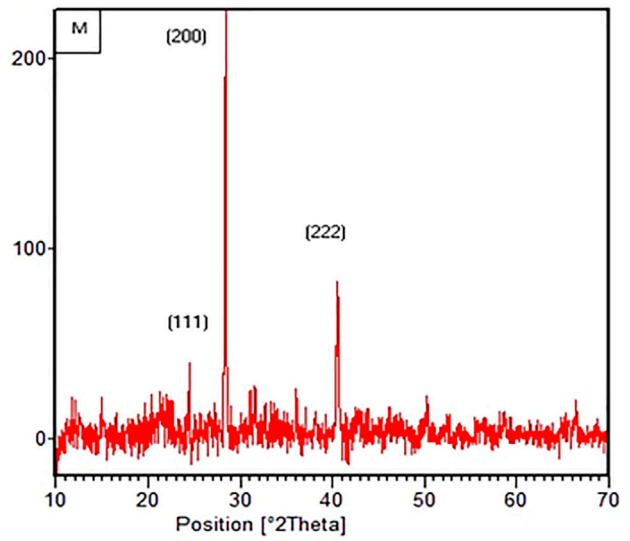

FIGURE 1 | X-ray diffraction spectroscopy of MgO nano-catalyst.

3 RESULTS AND DISCUSSION

3.1 Biodiesel Production

The transesterification was performed using MgO nano-catalyst to produce biodiesel.

Table 1 shows comprehensive experimental results of biodiesel synthesis reaction. For optimizing biodiesel yield (%), quadratic polynomial equation in terms of coded factors is as follow:

Biodiesel yield (wt: %) = +82.65 + 4.11 A + 2.67 B − 2.26 C − 2.12 D − 0.3125 AB − 0.6875 AC + 0.9375 AD + 1.69 BC + 0.0625 BD + 1.33 CD − 12.54 A^2 + 2.46 B^2 − 18.21 C^2 + 1.50 D^2

Table 2 shows the outcomes of the analysis of variance (ANOVA) for a quadratic model of RSM. ANOVA results depict a statistical correlation between four variables and biodiesel yield. *P*-value and F-value were calculated to find the corresponding coefficient's significance. The significance of the model is represented by a probability value (<0.05), and ANOVA results showing a *p*-value of 0.0087 declare the model significant, effectively predicting the biodiesel yield. Response values' accuracy prediction is measured by the coefficient of determination R^2. The predicted R^2 value was 0.6723, and the adjusted value of R^2 was 0.7741 (satisfactory) (**Table 2**). Quadratic term A^2 (met:oil) and C^2 catalyst loading is significant (*p*-value < 0.05) whereas B^2 reaction time and D^2 reaction temperature were found insignificant (*p*-value > 0.05). If these quadratic terms are excluded, then the quality of the model could be increased. However, model hierarchy is associated with these quadratic terms. Therefore, these are not excluded. According to the compulsion, the high precision value (6.2860) measures the ratio of signal to noise. A small lack of fit value (16.83) shows it is not considered comparable to pure error, deducing the significance of the model. The straight-line graph shows the close agreement between trial (experimental) and predicted yields, as depicted in **Supplementary Figure S3**.

3.2 Catalyst Characterization

3.2.1 X-ray Diffraction Spectroscopy of MgO

An XRD technique was used to determine the crystalline phase of the synthesized nano-catalyst. Peaks of different intensities were observed in MgO spectrum (**Figure 1**) to measure the crystalline shape and size. It was observed that peaks were being obtained at angles of 2θ. The diffraction peaks were observed at 38.40°, 42.22°, and at 63.07°, corresponding to (101), (102), and (103) planes, respectively (JCPDS-89-7746). Using the Debye Scherer, the average particle size was calculated.

$$D = \frac{K\ x\ \lambda\ (nm)}{FWHM \cos\theta} \tag{4}$$

where; D = crystalline size in nanometer; λ = wavelength in nanometer; FWHM = full width at half maximum and θ = Braggs angle θ

The average particle size was found to be 30 nm. XRD pattern of synthesized MgO proves the cubic structure of particles. Similar results were observed in the literature (Ashok et al., 2018; Shaheen et al., 2018). Foroutan and coworkers (2020) used MgO nano-catalyst for biodiesel production and found the diffraction peaks in similar spectrum patterns with particle sizes of 20–50 nm (Foroutan et al., 2020). Moreover, a similar cubic structure was observed by Lee and coworkers (2020) using a cubic f-MgO nano-catalyst; they also observed the peaks in similar 2θ regions, i.e., 36.9°, 42.9°, and at 62.2° (Lee et al., 2020). Rasouli and Esmaeili, 2019 found the nano-sized MgO catalyst of 5.5 nm. Dawood and coworkers 2018 used MgO nanoparticles of 70–90 nm size to convert yellow oleander into biodiesel. Similarly, MgO nano-catalyst with the size of 13 nm was synthesized by Shaheen and coworkers in 2018 and used to convert *Silybum eburneum* seed oil into biodiesel (Shaheen et al., 2018).

3.2.2 Scanning Electron Microscopy and Energy Dispersive X-ray Spectroscopy of MgO

SEM images of calcined MgO catalyst are shown in **Figures 2A–C** at different magnifications. It was observed that the catalyst has a porous lamellar-like smooth surface with particles of different sizes. There is also small particle agglomeration, which confirms the smaller particle size. SEM of MgO nano-catalyst shows a tighter, irregularly cubical structure with agglomerated nano entities. Du and coworkers reported the looser and more porous structure of MgO nano-catalyst (Du et al., 2019), while irregular morphology of varied sizes was reported by Dias et al. (2012). The chemical composition of the calcined catalyst was also observed by EDX analysis (**Figure 2D**). It shows 54.62% O, 30.72% Mg, 10.11% N, and 4.55% Al. The results indicate that the synthesized MgO catalyst has a high composition of two elements: oxygen and magnesium, as reported (Dawood et al., 2018).

3.2.3 Fourier Transform Infrared Spectroscopy Analysis of MgO Nano-catalyst

FTIR is performed to identify chemical bonds and characterize functional groups along with chemical bonds. FTIR spectrum

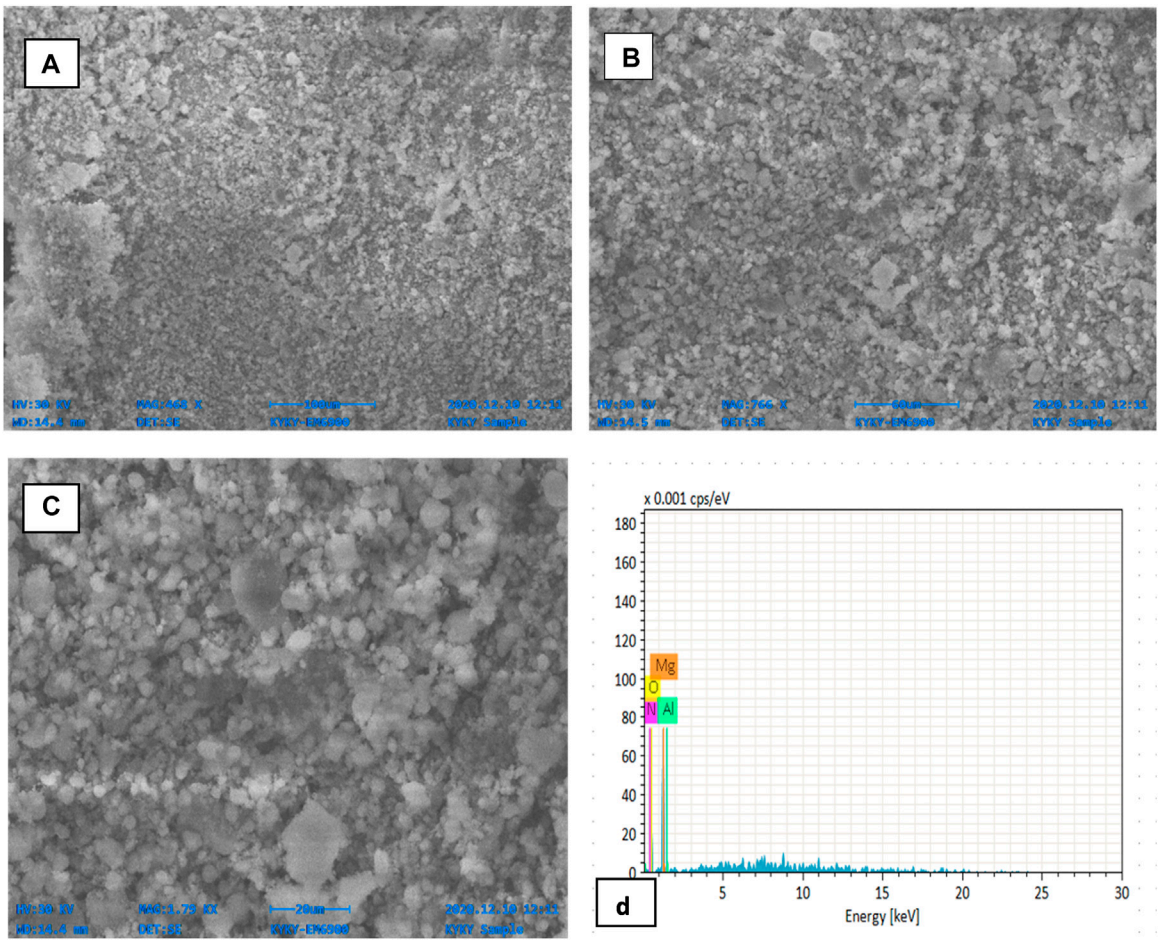

FIGURE 2 | SEM images of catalyst **(A,B,C)**, energy dispersive X-ray (EDX) spectrum of MgO **(D)**.

(**Figure 3**) depicts visible peaks such as 2981.08 cm^{-1} peak corresponding to C-H stretching vibrations. 1431.57 cm^{-1} peak corresponds to O-H bending vibrations. 1150.43 cm^{-1} corresponds to C-O stretching vibrations. 550.96 cm^{-1} peak corresponds to Mg-O vibrations. Tamilselvi et al., 2013 observed major peaks at 449 cm^{-1}, 511 cm^{-1}, 584 cm^{-1}, 671 $cm^{-1,}$ which confirmed the presence of Mg-O vibrations. In our study, a peak at 578.56 cm^{-1} is assigned to MgOH stretching vibration. 3,686 cm^{-1} sharp peak is absent because of anti-symmetric stretching vibrations in the crystal structure of $(MgOH)_2$ is further confirmation of calcination (600 ℃, 4 h), making cubic MgO from hexagonal $Mg(OH)_2$, as supported by previous studies (Shaheen et al., 2018).

3.3 Parametric Interactions of Biodiesel Synthesis Reaction

The synthesized MgO was used as a solid nano-catalyst to accomplish the transesterification of *Cucumis melo* var. *agrestis* seed oil for synthesizing FAME. The low acid value of 0.64 mg of KOH/g suggests a single-step, base-catalyzed transesterification reaction. The economically best amount of oil in seeds being used as feedstock should be 20%, and FFA content must be <3% to achieve high-rate conversion efficiency. However, FAME yield declines gradually in case of >3% subsequent in saponification, and eventually separation process turns out to be problematic.

3.3.1 Combined Effect of Methanol to Oil Molar Ratio and Catalyst Loading

A critical factor that influences the transesterification reaction is the alcohol-to-oil ratio. Response surface 3D plots were created from experimental data by using the design of experiment software. These response surface graphs depict the consequence of parametric interactions that affect biodiesel yield. Other optimization parameters were retained at their specific central points. **Figure 4A** shows the 3D graph of oil: methanol molar ratio with catalyst. The research reports expound 3 moles of alcohol react with a mole of triglycerides in oil, and 3 moles of fatty acid alkyl esters are produced due to transesterification reaction. A high yield of biodiesel can be achieved by using high alcohol content that produces triglyceride monoglycerides (Lam and Lee, 2011). Nevertheless, excess alcohol makes biodiesel purification difficult by enhancing glycerol solubility (Leung et al., 2010). Various studies depict

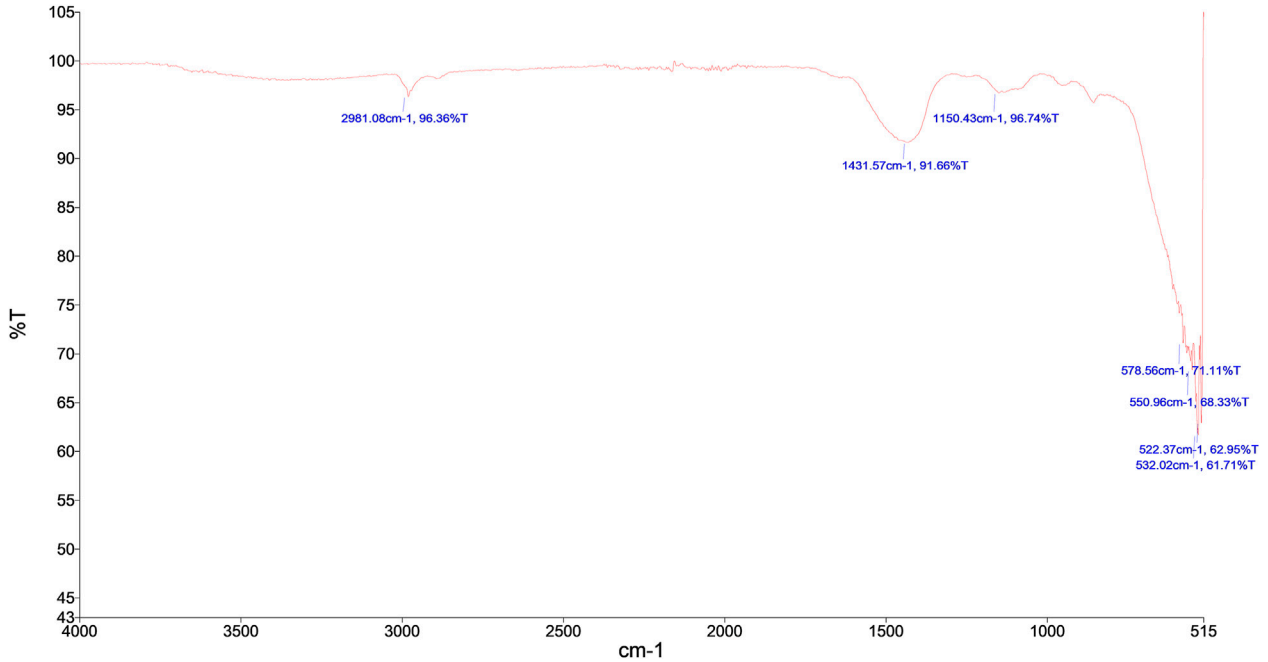

FIGURE 3 | FTIR spectra of MgO catalyst.

specific oil to methanol molar ratios to derive methanolysis (Kaur and Ali, 2014; Kostić et al., 2016; Teo, Rashid et al., 2014). The maximum FAME yield was 93% by increasing the molar ratio from 1:3 to 1:9 when the catalyst amount was 2%. The reason for an increase in yield may be attributed to the excess of methanol that refreshes the surface of catalysts and forms methoxy species that shifts the reaction to the forward direction (Moushoul et al., 2016). The yield of FAME was noticed to drop at molar ratios of oil to methanol higher than 1:9, which can be attributed to dilution of product and by-products like biodiesel and glycerol, respectively. It causes a shifting reaction in the reverse direction, consequently decreasing the yield (Musa, 2016). It is attributed that a rise in catalysts decreases the biodiesel yield because of the synthesis of unwelcome reaction products. Dilution of the catalyst due to methanol also interferes with the separation of glycerol from FAMEs, leading to low product yield.

3.3.2 Combined Effect of Catalyst Loading and Temperature

The collective influence of catalyst and temperature is given in **Figure 4B**. During the synthesis of FAMEs from seed oil, the catalyst amount was altered from 0.5 to 3.5% to study its impact on biodiesel yield under controlled reaction conditions having 1: 9 oil:methanol, at 90 °C and 360 min 3D plot of the effect of catalyst loading on biodiesel yield is shown in **Figure 4B**. It was observed that with the increase in catalyst from 0.5 wt% to 2 wt% of oil taken during transesterification, FAME yield was increased to 93%. The lowest FAME yield of 40% was obtained with catalyst 0.5 wt% as triglycerides converted into biodiesel partially (run 25). And the reaction temperature was 120 °C. While the maximum yield of methyl esters was obtained at 2 wt%, and this increase could be due to more active sites on the catalyst surface. The reaction temperature was 90 °C (run 26).

However, the additional catalyst concentration above it decreased the biodiesel yield probably because of an increase in viscosity of reaction mixture by the reduction in catalytic activity and, as a result lowering of interaction between catalyst and reaction medium leading to low product concentration (Musa, 2016). Hence, 2 wt% was noted as optimum catalyst loading to obtain maximum FAME yield via trans-esterification. An increase in yield of FAME of soybean oil was observed with an increase in MgO amount from 0.5 to 2%, but later, biodiesel yield was decreased with a further rise in concentration. Therefore, these results fully agree with the current research outcomes. An earlier study by Eevera and coworkers reports that further temperature increases leading to saponification results in low FAME yield (Eevera et al., 2009).

3.3.3 Collective Effect of Reaction Temperature and Time

Figure 4C depicts the collective effect of reaction temperature and time at constant oil to methanol molar ratio i.e. 1:9 and 2% catalyst. Like reaction temperature, the reaction time is another imperative parameter that affects the transesterification reaction as it specifies biodiesel production cost. The collective effect is represented as 3D plot in **Figure 4C**. The reaction time of 60–360 min has been noticed in this communication. FAME yield was increased considerably to 93% after 360 min at 90°C and further increase from optimum time led to a sudden drop in yield. It can be justified that chemical equilibrium was not

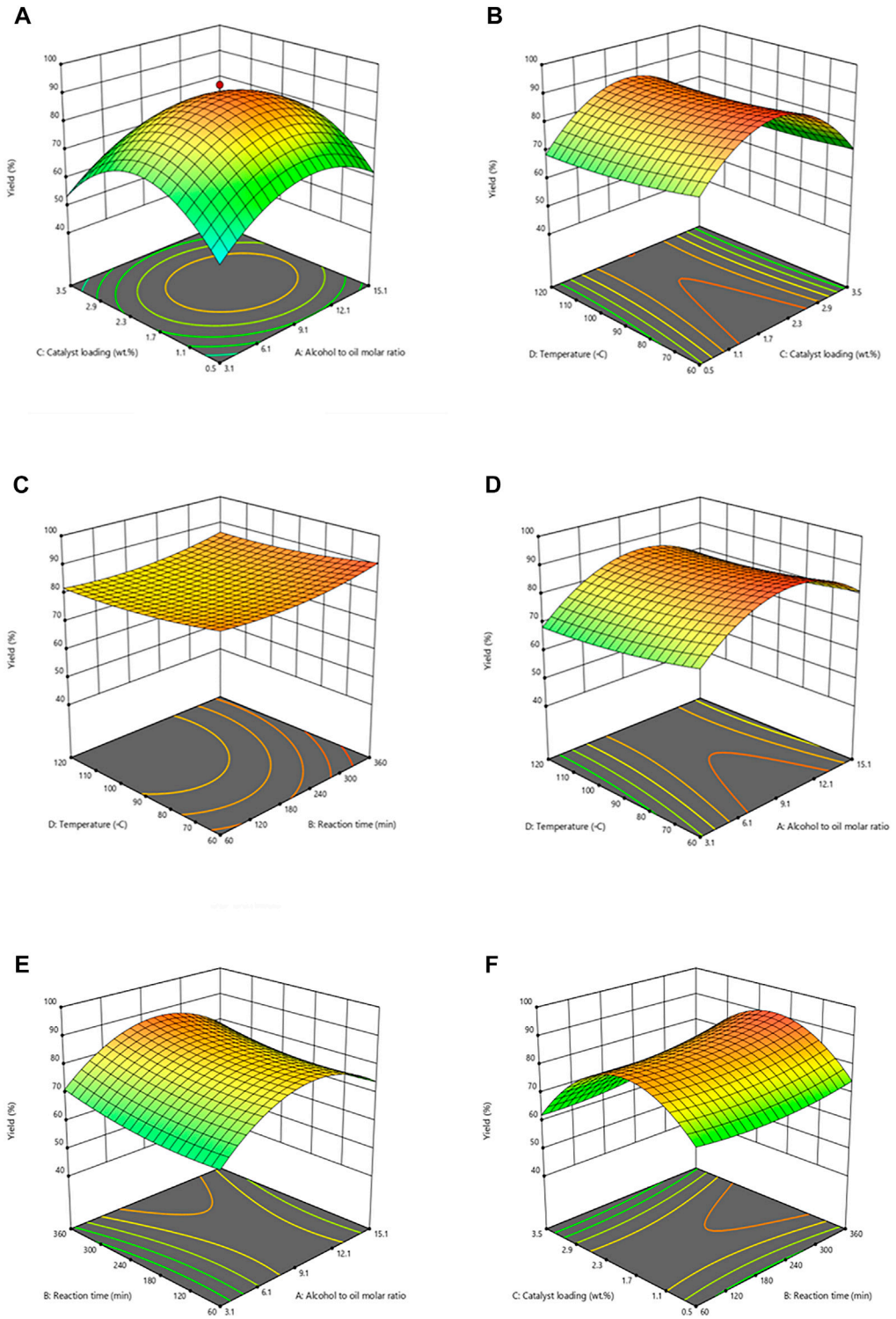

FIGURE 4 | Influence of reaction parameters on *Cucumis melo* var. *agrestis* biodiesel. **(A)** Catalyst loading vs alcohol to oil molar ratio, **(B)** Temperature vs catalyst loading, **(C)** Temperature vs reaction time, **(D)** Temperature vs alcohol to oil molar ratio, **(E)** Reaction time vs alcohol to oil molar ratio, and **(F)** Catalyst loading vs reaction time.

attained within 1 hour of reaction time because all reactants could not find enough time for interaction with the catalyst, leading to a lower product. It is clear that at 9:1 methanol to oil molar ratio, 2 wt% catalysts at 90°C for 60 min, the yield was 70% (run 22), and decreased yield is attributed to less time duration and insufficient time required to achieve maximum yield and increase in time to 210 min increased yield to 89% (run 20). In optimum time duration (360 min), the reaction moved forward, equilibrium was achieved, and maximum yield, i.e., 93%, was observed (run 26). However, further increase in time did not increase FAME yield. However, a slight reduction in products was observed in longer hours of reaction time as conversion to reactants occurred in backward reaction. Several studies have reported the effect of reaction time on biodiesel yield (Eevera et al., 2009). Various studies reported the effect of reaction time on product yield (Okwundu et al., 2019). For instance, constant elevation in FAME yield was noted with an increase in reaction time, increasing yield, and after a specific time, it decreases due to reversible transesterification reaction.

3.3.4 Combined Effect of Oil to Methanol Molar Ratio and Reaction Temperature

Within the specific optimum range, high temperature enhances the reaction rate as it significantly impacts the biodiesel synthesis process. Various research indicates that a high yield is obtained within the range of 60–70℃ (Deshmane & Adewuyi, 2013). **Figure 4D** is 3D plot of the influence of reaction time on esters production at constant catalyst loading at 2 wt% and 360 min reaction time. During transesterification using MgO (2% w/w) for 3 h, different temperatures were selected accordingly to check out its effect on FAME yield. Results of experimental work indicate that a gradual temperature rise has a pronounced impact on the rate of reaction, but after a certain limit, it decreases. The optimum temperature for transesterification was 90℃, and the reason for the rise in reaction rate at elevated temperature is owing to the lowering of activation energy resulting in increased interaction between catalyst and reactants, leading to the higher conversion into products. Nevertheless, a considerable reduction in products was seen with a further increase over the optimum temperature. This is perhaps because of the evaporation of methanol above the threshold temperature (90℃), resulting in little biodiesel yield. Lower temperature results in lower yields that are attributed to the reduced mass transfer rate of oil, methanol, and catalyst, as they all are immiscible at lower temperatures and need sufficient kinetic energy to react appropriately and increase productivity in a shorter period. It is determined from the current study that combining the effect of molar ratio and temperature is worthy of being considered during transesterification reaction.

3.3.5 Combined Effect of Oil to Methanol Molar Ratio and Reaction Time

The oil to methanol molar ratio and reaction time is another critical reaction parameter that considerably affects biodiesel yield. **Figure 4E** depicts the combined effect of oil to methanol molar ratio 1) and reaction time 2), while other reaction variables like temperature (90°C) and catalyst loading (2 wt%) were kept constant. A maximum yield of 93% was observed at a 1:9 M ratio and a time of 360 min. It can be credited with enhancing the interaction of excess methanol with triglycerides for a long duration. However, a lesser time of transesterification (210 min) with low molar ratio leads (3:1) to comparatively slighter biodiesel yield, i.e., 55% (run 29). It is most possibly due to insufficient time for the reactants to react properly, resulting in the incomplete conversion of reactants into products. Reduction in the biodiesel yield (78%) was observed at higher oil to methanol ratio of 1:15 with time 210 min at run number due to the excess amount of methanol, which shifted reaction toward unwanted reaction condition, facilitating reverse reaction and subsequent low yield of biodiesel.

3.3.6 Combined Effect of Reaction Time and Catalyst Loading

Figure 4F depicts the collective effect of reaction time (B) and catalyst loading (C) for transesterification in the form of 3D plots while keeping other reaction parameters constant. A maximum yield of 93% was obtained at the optimum time (360 min) and catalyst amount (2%) at run 26 due to equilibrium in the transesterification reaction. The optimal level reaction time (from360 min to 210 min) and catalytic amount decrease in biodiesel yield were also noted. A short time (210 min) rendered biodiesel yield (70%) when optimum conditions were provided, i.e., 1:9 oil to methanol molar ratio, a 2 wt% catalyst, and 90°C temperature (run 22). In the same time duration, i.e., 210 min, 9:1 M ratio, 90°C temperature, yielded considerably low biodiesel yield (65%) at a high amount of catalyst due to partial conversion of reactant into products (run 18).

3.4 Characterization of Biodiesel

3.4.1. Gas Chromatography and Mass Spectroscopy

To check the chemical composition produced, biodiesel was processed through gas chromatography and mass spectroscopy (GC- MS). Seven major peaks in the biodiesel sample were observed with library software (NO. NIST02) (**Figure 5**). The quantified FAMEs include octanoic acid, methyl ester, methyl 8-oxooctanoate, nonanoic acid, 9-oxo, methyl ester, dodecanoic acid, methyl ester, 10-oxodecanoic acid, methyl ester, cyclopropaneoctanoic acid, 2- hexyl methyl ester, 2-(3-oxocyclohexyl) thio propionic acid (**Figure 5**). The engine clogging occurs due to acceleration of peroxidation at high temperatures. Hence, a biodiesel feedstock with a high polyunsaturated level is considered unfeasible. Moreover, mono-unsaturated acids do not have an affinity for oxygen, causing peroxidation. These primary methyl esters have already been reported in previous studies (Kanakdande and Khobragade, 2020; Laskar et al., 2020).

3.4.2 Fourier Transform Infrared Spectroscopy

FTIR is an advanced technique involving infrared radiations to detect chemical bonds and functional groups in each compound (Rizwanul Fattah et al., 2020). In the current study, the

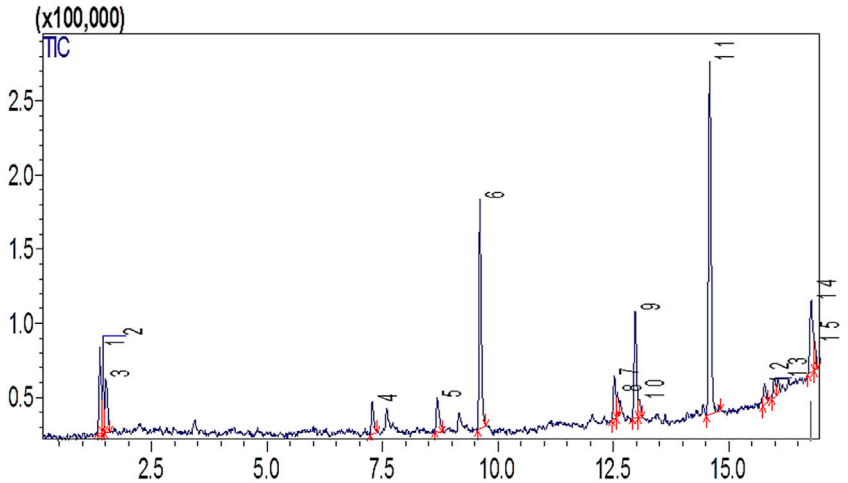

FIGURE 5 | GC-MS analysis of *Cucumis melo* var. *agrestis* biodiesel.

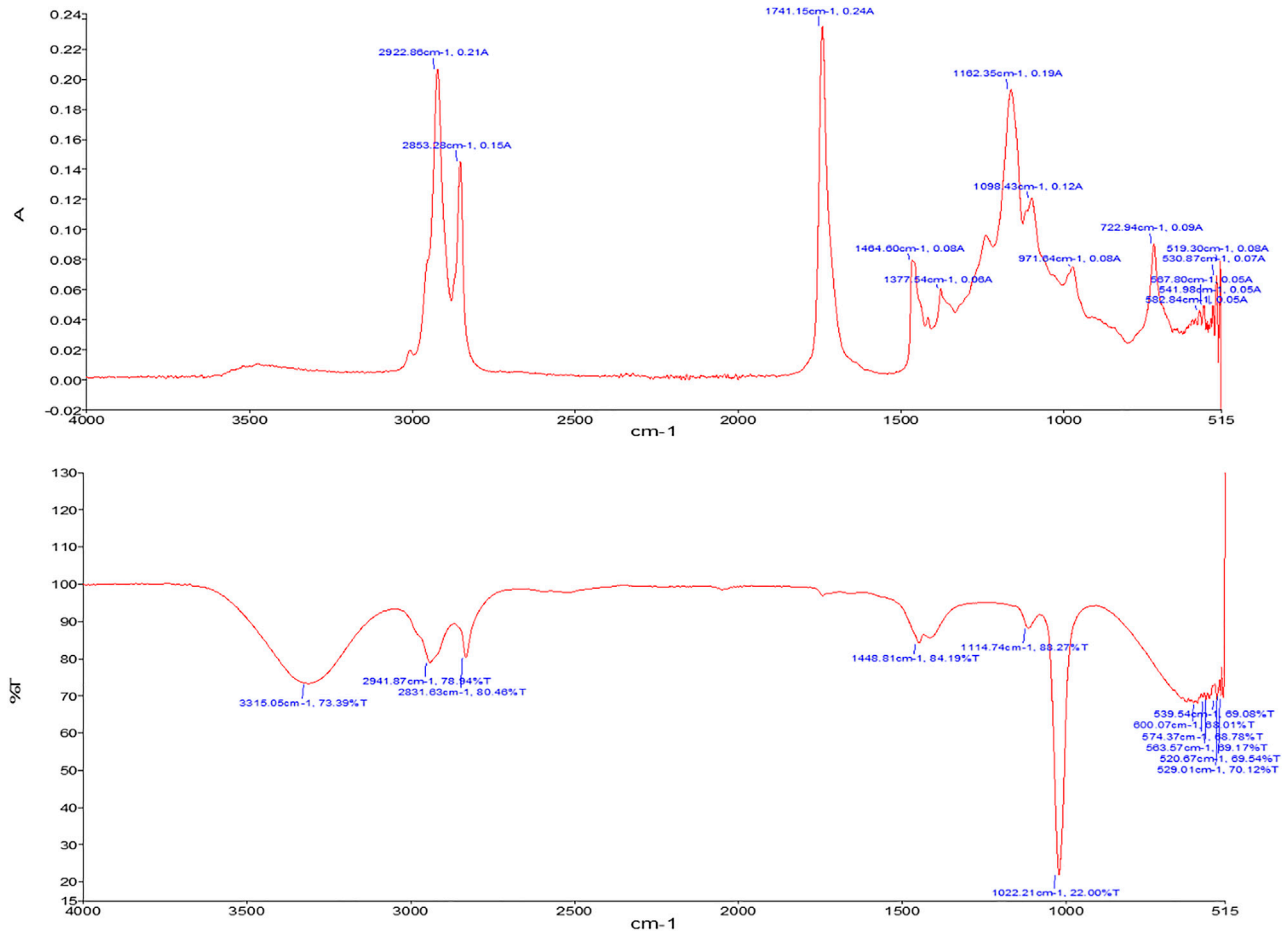

FIGURE 6 | FT-IR spectrum of *Cucumis melo* var. *agrestis* oil (upper), biodiesel (lower).

TABLE 3 | FTIR of oil extracted from *Cucumis melo* var. *agrestis* seed.

Sr No.	Peak (cm^{-1})	Absorbance (%)	Transmittance	Bond stretch	Range (cm^{-1})	Functional Group
1	2922.86	0.21	61.6	C-H stretching	3,000–2840	Alkane
2	2853.28	0.15	0.79	C-H stretching	3,000–2840	Alkane
3	1741.15	0.24	57.54	C=O Stretching	1750–1735	Esters
4	1464.60	0.08	83.17	C-H bending	1465	Methyl group
5	1377.54	0.08	83.17	O-H bending	1390–1310	Phenol
6	1162.35	0.19	64.56	C=O stretching	1210–1163	Esters
7	1098.43	0.12	75.85	C-O stretching	1085–1085	Secondary alcohol

TABLE 4 | FTIR of *Cucumis melo* var. *agrestis* biodiesel.

Sr No.	Peak (cm^{-1})	Transmittance (%)	Bond stretch	Range (cm^{-1})	Functional Group
1	3,315.05	73.39	N-N stretching	3,350–3,310	Secondary amine
2	2941.87	78.94	C-H stretching	3,000–2840	Alkane
3	2831.63	80.46	C-H stretching	2830–2695	Aldehyde
4	1448.81	84.19	C-H stretching	1450	Methyl group
5	1114.74	88.27	C=O stretching	1210–1163	Ester
6	1022.21	22.00	C-N stretching	1250–1020	Amine

composition of oil and biodiesel was analyzed by sample scanning in mid-IR region, i.e., 400–4,000 $cm^{-1,}$ and characteristic peaks of specific molecular bonds were observed. The FTIR spectra of crude oil are depicted, and prepared biodiesel is shown in **Figure 6**. When two spectra are compared, peaks at 2922.86 cm^{-1} and 2853.28 cm^{-1} in *Cucumis melo* var. *agrestis* oil corresponds to C-H stretching bonds of triglycerides (**Figure 6**) In contrast, the esters group (C=O stretching) of triglyceride was observed at 1741.15 cm^{-1} and 1162.35 cm^{-1} peaks (**Table 3**). However, in biodiesel, FAMEs were confirmed by peaks at 2941.87 cm^{-1} corresponding alkane, 1448.81 cm^{-1} (C-H stretching) corresponding to the methyl group. The major difference in both spectra is the appearance of a 1114.74 cm^{-1} peak (C=O stretching) corresponding to the ester group that confirms the biodiesel (**Table 4**).

3.4.3 Nuclear Magnetic Resonance Study

3.4.3.1 H^1Nuclear Magnetic Resonance Spectroscopy

This study involved the potential of H^1NMR to evaluate fuel properties for *Cucumis melo* var. *agrestis* biodiesel. **Figure 7** (upper) depicts the characteristic peaks of H^1NMR spectrum. A characteristic singlet peak at 3.655 ppm represents the methoxy protons (-OCH_3), and hence FAME synthesis from oil has been confirmed. Peaks in the range of 3.3–4.1 showed aliphatic hydrogen and alkoxy groups that confirm esters' presence. On transesterification, triglyceride is converted into respective alkyl ester depending on the alcohol used, and glycerol part on substitution with alcohol results in the appearance of an NMR signal ranging between 5.3–3.3 ppm. Faraguna et al. (2017) observed peaks of H^1NMR spectra ranging from 4.3 to 3.5 ppm with assigned biodiesel and protons of different alcohols used to produce biodiesel. A distinctive peak that appeared at 3.6 shows the presence of hydrogen adjacent to the electronegative atom in the biodiesel spectrum corresponding to methoxy (-OCH_3) (**Figure 7** upper). Previous studies are evidence of the presence of methoxy at this position (Joseph et al., 2010; Faraguna et al., 2017; Dawood et al., 2018; Munir et al., 2020; Ullah et al., 2020). Other conspicuous peaks include 0.876–0.884 ppm showing terminal methyl protons (–CH_3), 2.033–2.786 ppm α-methylene protons (–CH_2), 1.252–1.636 ppm for β-methylene protons (–CH_2), 5.322–5.350 ppm depicts Olefinic protons (–HC=CH), respectively. These detected signals indicate different methyl esters present in the biodiesel sample, as mentioned in (**Table 5**).

3.4.3.2 ^{13}C Nuclear Magnetic Resonance Spectroscopy

The ^{13}C NMR spectroscopy is an unsurpassed analytical technique to study the structural characterization of FAMEs and their spectrum. The ^{13}C NMR spectrum is shown in **Figure 7** (lower), in which the signals of 51.35 and 174.21 ppm, depict the characteristic ester methoxy carbon (–OMe) and carbonyl group (-COOR), respectively, as shown in **Figure 7** (lower). These detected signals indicate the presence of different carbons in methyl esters present in the biodiesel sample, as mentioned in **Table 6**. Peaks appeared at 130.13, and 127.07 ppm show the unsaturated double bonds (C=C) in methyl esters. However, a peak at 14.03 depicts terminal carbon of methyl groups (–CH_3), and 25.59–34.04 ppm shows the long carbon's ethylene carbons (–CH2–). Our results agree with ^{13}CNMR spectrum of sunflower oil and fatty acid ester by Li et al. (2017) and coincide with NMR spectroscopy of yellow oleander biodiesel (Dawood et al., 2018; J.; Li et al., 2017; 2020).

4 FUEL PROPERTIES

The fuel properties of synthesized biodiesel were determined and compared with ASTM standards. Fuel properties like total acid no.,

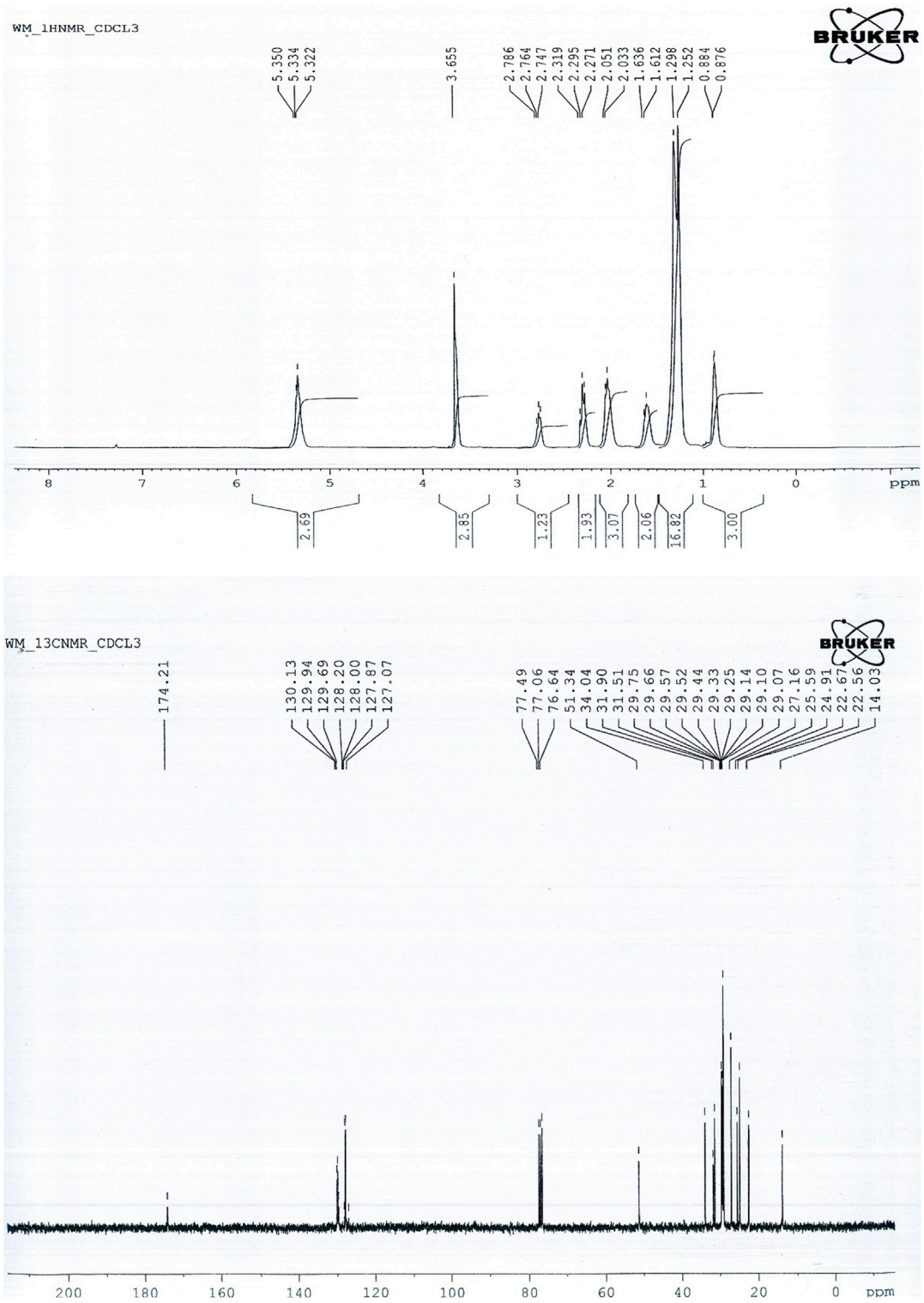

FIGURE 7 | H^1NMR (upper), and C^{13} NMR (lower) spectrum of *Cucumis melo* var. *agrestis* biodiesel.

TABLE 5 | H^1NMR spectrum of *Cucumis melo* var. *agrestis* biodiesel.

Peak/No.	Peak Area Region (ppm)	Identified Compounds	Chemical Formula
1	0.876–0.884	Terminal methyl protons	$–CH_3$
2	1.252–1.636	β-methylene protons	$–CH_2$
3	2.033–2.786	α-methylene protons	$–CH_2$
4	3.655	methoxy proton	$–OCH_3$
5	5.322–5.350	Olefinic protons (unsaturated)	–HC = CH

TABLE 6 | C13 NMR spectrum of *Cucumis melo* var. *agrestis* biodiesel.

Peak/No.	Peak Area Region (ppm)	Identified Compounds	Chemical Formula
1	14.03	Terminal methyl carbon	$–CH_3$
2	22.56–34.04	methylene carbon	$–CH_2$
3	51.34	methoxy carbon	$–OCH_3$
4	127.07–130.13	Olefinic carbons (unsaturation)	C=C
5	174.21	Carbonyl carbon of esters	$-COOCH_3$

TABLE 7 | Fuel properties of *Cucmis melo* var. *agrestis* biodiesel.

Tests	Method	Results	ASTM standard
Color	ASTM D-1500	Visual	2
Flash Point ℃ (PMCC)	ASTM D-93	73.5	60–100
Density @15□C kg/L	ASTM D-1298	0.800	0.8–0.9
K. Viscosity @ 40□C cSt	ASTM D-445	4.23	1.9–6.0
Pour Point □C	ASTM D-97	-7	-15–16
Cloud Point □C	ASTM D-2500	-12	-3–12
Sulphur % wt	ASTM D-4294	0.0001	0.05
Total Acid No. mg KOH/gm	ASTM D-974	0.167	0.5

Rasouli, H., & Esmaeili, H. (2019). Characterization of MgO nano-catalyst to produce biodiesel from goat fat using transesterification process. 3 Biotech, 9*(11), 1-11.*

flash point, sulfur content, cloud point, kinematic viscosity, pour point, and density was investigated (Hasan et al., 2015; Akhtar et al., 2019; Mallah & Sahito, 2020). According to ASTM standards, the color of *Cucumis melo* var. *agrestis* biodiesel is visual. On exposure to a spark or flame, an ignitable mixture is formed by a liquid at a specific lowest temperature in the air vicinity of that liquid. This flashpoint gives the measurement of the capacity of liquid to form a combustible blend. When fuel is needed to be shifted, stored, or handled for usability, it is safe if it partakes high flash points (Dawood et al., 2021). The recorded value as (73.5℃) using ASTM- 93 of the sample shows that the fuel is safe to use, as diesel has a flashpoint 53℃, and the range 60–80℃ shows the flashpoint of high-speed diesel (HSD). Mass per unit of the volume that measures in a vacuum is known as the density of the fuel. Biodiesel quality can be easily assessed by checking out density because fuel efficiency is directly affected by density, which is strongly linked to cetane number and viscosity. ASTM D-1298 was standard for the determination of biodiesel density that was found as 0.800 kg/L whereas the density of HSD is 0.834 kg/L. Hence *Cucumis melo* var. *agrestis* biodiesel has less density as compared to HSD. It acts as a sign to show the capability of the liquid to run (**Table 7**).

The high viscosity of fuel severely influences engine efficiency. Instead of directly using highly viscous crude oil, lowering their viscosity via the esterification process has become indispensable and expedient. The viscosity of vegetable oil is 27.2–53.6 mm^2/s, whereas the viscosity of biodiesel produced from them is 3.6–4.6 mm^2/s. Less viscous oil is required for easy drainage and to get very fine droplets of fuel (Mustapha et al., 2019; Razavi et al., 2019). According to ASTM D-445 standards, the kinematic viscosity of *Cucumis melo* var. *agrestis* biodiesel is 4.23 @ 40℃. Biodiesel of rapeseed oil and palm oil biodiesel is 4.2 and 4.3–4.5 @ 40□C, respectively, similar to or higher than the kinematic viscosity of *Cucumis melo* var. *agrestis* biodiesel. As K. Viscosity (4.23 mm^2/s) lies between the standards values (i.e., 1.9–6.0 mm^2/s). In chilled conditions, the minimum temperature at which crystallization of paraffin or its tendency to be separated in ice-cold in proposed conditions is known as cloud point (Dunn, 2021). The temperature that allows fuel to flow is called the pour point. Saydut and coworkers reported both parameters as −6℃, and −14℃, respectively, in biodiesel produced from sesame seed oil (Saydut et al., 2008). In the current study, the determination of cloud point and pour point was carried out using ASTM D-2500 and ASTM D-97 standards.

According to ASTM standards, the value of the pour point was −7□C, and its cloud point was −12□C, higher than HSD. In polluted areas, the fuel having fewer sulfur contents is considered ideal. Low sulfur content is indispensable for the environment and the engine's life (Hoang et al., 2019). Therefore, the sulfur content in *Cucumis melo* var. *agrestis* biodiesel is 0.0001 by weight which is low according to ASTM D- 4,292 standard, i.e., 0.05. Due to its decreasing no. of sulfur amount proves that the biodiesel is super than HSD. Acid or neutralization number is the amount of carboxylic acid utilized or the presence of FFA in the sample of fuel taken as mg KOH/gm required to neutralize FAME (1 g). It specifies the

confirmation of accurate fuel's aging property and/or a proper synthesis procedure and fuel degradation due to thermal degradation. FFA content results in elevation of acidity of diesel fuel; otherwise, diesel has no acidic nature. The high number of acid values affects the engine efficiency. It causes corrosion in the system and inside the engine functions. The acid value of *Cucumis melo* var. *agrestis* biodiesel is 0.167, which lies within limits (0.5) of international standards of ASTM D-974.

5 CATALYST REUSABILITY

After transesterification, the synthesized solid nano-catalyst (MgO) can be separated from reaction media to access catalyst reusability. Optimized reaction conditions (9:1 methanol oil, 2 wt% catalysts at 90℃) were used to investigate the extent of catalyst reusability during the reaction (**Supplementary Figure S4**). The spent catalyst was reused by filtration and washing with methanol, followed by catalyst drying (100℃ up to 4 h). In the present study, the MgO nano-catalyst was successfully reused 5 times without declining its catalytic ability. During the first 4 rounds, there was a slight drop in biodiesel yield (93–89.9%). Afterward, there was a sudden drop in biodiesel yield (87.5% fifth run) because of catalyst deactivation. There could be due to surface poisoning, leaching of active sites, structure collapse, or pore filling.

6 CONCLUSIONS

The current study synthesizes and applies green nano-catalyst (MgO) to convert *Cucumis melo* var. *agrestis* seed oil to biodiesel. A maximum biodiesel yield of 93% was achieved under optimized operating parameters (9:1 methanol:oil, 2 wt% catalysts at 90℃). RSM built on the BBD was used to optimize the biodiesel yield. The fuel properties of synthesized biodiesel (density 0.800 kg/L, kinetic viscosity @ 40 □C 4.23 cSt, cloud point −12°C, pour point −7°C, sulfur content 0.0001%, flash point 73.5°C, total acid no. 0.167 mg KOH/g) meets with the international stand]ard of ASTM. In general, *Cucumis melo* var. *agrestic* seed oil and nano MgO catalyst appeared as economical, sustainable, and feasible candidates to overcome global energy glitches and environmental issues. Using MgO catalyst, non-edible *Cucumis melo* var. *agrestis* seed oil could be a potential candidate for sustainable bioenergy production.

DATA AVAILABILITY STATEMENT

The original contributions presented in the study are included in the article/**Supplementary Material**. Further inquiries can be directed to the corresponding author.

AUTHOR CONTRIBUTIONS

MA: conceptualization, writing-original Draft; MZ: design review, implementation; AN: supervision, validation, review-editing; MA: supervision, review-editing; MM: visualization, formal analysis; SS: resources; AU: resources; MR: verification, editing.

FUNDING

This work was financially supported by Higher Education Commission (Ref No. SRGP No. 10767/IPFP-II (Batch-I)/ SRGP/NAHE/HEC/2020/300).

SUPPLEMENTARY MATERIAL

The Supplementary Material for this article can be found online at: https://www.frontiersin.org/articles/10.3389/fenrg.2022.830845/full#supplementary-material

REFERENCES

Ahmad, A. L., Yasin, N. H. M., Derek, C. J. C., and Lim, J. K. (2011). Microalgae as a Sustainable Energy Source for Biodiesel Production: a Review. *Renew. Sustain. Energy Rev.* 15 (1), 584–593. doi:10.1016/j.rser.2010.09.018

Ahmad, M., Ahmed, S., Riaz, M. A., Zafar, M., Khan, M. A., and Sultana, S. (2011a). Strategy for the Supply Chain Development of Biodiesel as an Alternative Fuel in Pakistan. *Energy Sources, Part B Econ. Plan. Policy* 6 (3), 220–227. doi:10.1080/15567249.2010.536814

Ahmad, M., Samuel, S., Zafar, M., Khan, M. A., Tariq, M., Ali, S., et al. (2011b). Physicochemical Characterization of Eco-Friendly Rice Bran Oil Biodiesel. *Energy Sources, Part A Recovery, Util. Environ. Eff.* 33 (14), 1386–1397. doi:10.1080/15567036.2010.511428

Ahmad, M., Sultana, S., Keat Teong, L., Abdullah, A. Z., Sadia, H., Zafar, M., et al. (2015). Distaff Thistle Oil: a Possible New Non-edible Feedstock for Bioenergy. *Int. J. Green Energy* 12 (11), 1066–1075. doi:10.1080/15435075.2014.891220

Ahmad, M., Ullah, K., Khan, M. A., Zafar, M., Tariq, M., Ali, S., et al. (2011c). Physicochemical Analysis of Hemp Oil Biodiesel: a Promising Non Edible New Source for Bioenergy. *Energy Sources, Part A Recovery, Util. Environ. Eff.* 33 (14), 1365–1374. doi:10.1080/15567036.2010.499420

Ahmad, M., Zafar, M., Azam, A., Sadia, H., Khan, M. A., and Sultana, S. (2011d). Techno-economic Aspects of Biodiesel Production and Characterization. *Energy Sources, Part B Econ. Plan. Policy* 6 (2), 166–177. doi:10.1080/15567249.2010.529557

Ahmad, M., Zafar, M., Sultana, S., Khan, M. A., Hasan, A., Riaz, M. A., et al. (2013). Policy Recommendation for Renewable Energy from Biofuels. *Energy Sources, Part B Econ. Plan. Policy* 8 (1), 67–75. doi:10.1080/15567249.2011.569832

Akhtar, M. T., Ahmad, M., Shaheen, A., Zafar, M., Ullah, R., Asma, M., et al. (2019). Comparative Study of Liquid Biodiesel from Sterculia Foetida (Bottle Tree) Using CuO-CeO_2 and Fe_2O_3 Nano Catalysts. *Front. Energy Res.* 7, 4. doi:10.3389/fenrg.2019.00004

Akia, M., Yazdani, F., Motaee, E., Han, D., and Arandiyan, H. (2014). A Review on Conversion of Biomass to Biofuel by Nanocatalysts. *Biofuel Res. J.* 01 (1), 16–25. doi:10.18331/BRJ2015.1.1.5

Alhassan, F. H., Rashid, U., and Taufiq-Yap, Y. H. (2015). Synthesis of Waste Cooking Oil-Based Biodiesel via Effectual Recyclable Bi-functional $Fe_2O_3MnOSO_4^{2-}/ZrO_2$ Nanoparticle Solid Catalyst. *Fuel* 142, 38–45. doi:10.1016/j.fuel.2014.10.038

Ameen, M., Ahmad, M., Zafar, M., and Sultana, S. (2021). Oil Extraction Techniques for Bioenergy Production: a Systematic Review. *JBBT* 1 (1).

Ameen, M., Zafar, M., Ahmad, M., Shaheen, A., and Yaseen, G. (2018). Wild Melon: a Novel Non-edible Feedstock for Bioenergy. *Pet. Sci.* 15 (2), 405–411. doi:10.1007/s12182-018-0227-0

Antero, R. V. P., Alves, A. C. F., de Oliveira, S. B., Ojala, S. A., and Brum, S. S. (2020). Challenges and Alternatives for the Adequacy of Hydrothermal Carbonization of Lignocellulosic Biomass in Cleaner Production Systems: a Review. *J. Clean. Prod.* 252, 119899. doi:10.1016/j.jclepro.2019.119899

Ashok, A., Kennedy, L. J., Vijaya, J. J., and Aruldoss, U. (2018). Optimization of Biodiesel Production from Waste Cooking Oil by Magnesium Oxide Nanocatalyst Synthesized Using Coprecipitation Method. *Clean. Techn Environ. Policy* 20 (6), 1219–1231. doi:10.1007/s10098-018-1547-x

Babu, B. S., Kumar, D. B., Sathiyaraj, S., and senthilkumar, A. (2020). Experimental Investigation and Performance of Diesel Engine Using Biodiesel Coriander Seed Oil. *Mater. Today Proc.* 33, 1044–1048. doi:10.1016/j.matpr.2020.07.055

Bet-Moushoul, E., Farhadi, K., Mansourpanah, Y., Nikbakht, A. M., Molaei, R., and Forough, M. (2016). Application of CaO-based/Au Nanoparticles as Heterogeneous Nanocatalysts in Biodiesel Production. *Fuel* 164, 119–127. doi:10.1016/j.fuel.2015.09.067

Callegari, A., Bolognesi, S., Cecconet, D., and Capodaglio, A. G. (2020). Production Technologies, Current Role, and Future Prospects of Biofuels Feedstocks: A State-Of-The-Art Review. *Crit. Rev. Environ. Sci. Technol.* 50 (4), 384–436. doi:10.1080/10643389.2019.1629801

Cavalheiro, L. F., Rial, R. C., de Freitas, O. N., Domingues Nazário, C. E., and Viana, L. H. (2021). Thermal Cracking of Fodder Radish (Raphanus Sativus L.) Oil to Use as Biofuel. *J. Anal. Appl. Pyrolysis* 157, 105223. doi:10.1016/j.jaap.2021.105223

Cheema, S. I., Ahmad, M., Ullah, R., Mothana, R. A., Noman, O. M., Zafar, M., et al. (2021). Implication, Visualization, and Characterization through Scanning Electron Microscopy as a Tool to Identify Non-edible Oil Seeds. *Microsc. Res. Tech.* 84 (3), 379–39321. doi:10.1002/jemt.23595

Dai, J., Chen, B., Hayat, T., Alsaedi, A., and Ahmad, B. (2015). Sustainability-based Economic and Ecological Evaluation of a Rural Biogas-Linked Agro-Ecosystem. *Renew. Sustain. Energy Rev.* 41, 347–355. doi:10.1016/j.rser.2014.08.043

Dawood, S., Ahmad, M., Ullah, K., Zafar, M., and Khan, K. (2018). Synthesis and Characterization of Methyl Esters from Non-edible Plant Species Yellow Oleander Oil, Using Magnesium Oxide (MgO) Nano-Catalyst. *Mater. Res. Bull.* 101, 371–379. doi:10.1016/j.materresbull.2018.01.047

Dawood, S., Ahmad, M., Zafar, M., Ali, M. I., Ahmad, K., Sultana, S., et al. (2020). Identification of Novel Nonedible Oil Seeds via Scanning Electron Microscopy for Biodiesel Production. *Microsc. Res. Tech.* 83 (2), 165–17525. doi:10.1002/jemt.23399

Dawood, S., Koyande, A. K., Ahmad, M., Mubashir, M., Asif, S., Klemeš, J. J., et al. (2021). Synthesis of Biodiesel from Non-edible (Brachychiton Populneus) Oil in the Presence of Nickel Oxide Nanocatalyst: Parametric and Optimisation Studies. *Chemosphere* 278, 130469. doi:10.1016/j.chemosphere.2021.130469

Deshmane, V. G., and Adewuyi, Y. G. (2013). Synthesis and Kinetics of Biodiesel Formation via Calcium Methoxide Base Catalyzed Transesterification Reaction in the Absence and Presence of Ultrasound. *Fuel* 107, 474–482. doi:10.1016/j.fuel.2012.12.080

Dias, A. P. S., Bernardo, J., Felizardo, P., and Correia, M. J. N. (2012). Biodiesel Production by Soybean Oil Methanolysis over SrO/MgO Catalysts. *Fuel Process. Technol.* 102, 146–155. doi:10.1016/j.fuproc.2012.04.039

Du, L., Li, Z., Ding, S., Chen, C., Qu, S., Yi, W., et al. (2019). Synthesis and Characterization of Carbon-Based MgO Catalysts for Biodiesel Production from castor Oil. *Fuel* 258, 116122. doi:10.1016/j.fuel.2019.116122

Dunn, R. O. (2021). Correlating the Cloud Point of Biodiesel with its Fatty Acid Methyl Ester Composition: Multiple Regression Analyses and the Weighted Saturation Factor (wSF). *Fuel* 300, 120820. doi:10.1016/j.fuel.2021.120820

Eevera, T., Rajendran, K., and Saradha, S. (2009). Biodiesel Production Process Optimization and Characterization to Assess the Suitability of the Product for Varied Environmental Conditions. *Renew. Energy* 34 (3), 762–765. doi:10.1016/j.renene.2008.04.006

Esmaeili, H., Yeganeh, G., and Esmaeilzadeh, F. (2019). Optimization of Biodiesel Production from Moringa Oleifera Seeds Oil in the Presence of Nano-MgO Using Taguchi Method. *Int. Nano Lett.* 9 (3), 257–263. doi:10.1007/s40089-019-0278-2

Faostat (2017b). *FAO Statistical Databases Data Sets*. Available at: http://www.fao.org/faostat/en/#data (accessed on July 15, 2019).

Faostat (2017a). *Food and Agriculture Organization of the United Nations*. FAO. Retrieved from http://www.fao.org/faostat/en/#data/QC(accessed on may 1, 2021)

Faraguna, F., Racar, M., Glasovac, Z., and Jukić, A. (2017). Correlation Method for Conversion Determination of Biodiesel Obtained from Different Alcohols by 1H NMR Spectroscopy. *Energy fuels.* 31 (4), 3943–3948. doi:10.1021/acs.energyfuels.6b02855

Food and Agriculture Organization of the United Nations (2013). *FAO Year Book Production*. Rome. Retrieved from: www.faostat.fao.org.

Foroutan, R., Mohammadi, R., Esmaeili, H., Mirzaee Bektashi, F., and Tamjidi, S. (2020). Transesterification of Waste Edible Oils to Biodiesel Using Calcium Oxide@magnesium Oxide Nanocatalyst. *Waste Manag.* 105, 373–383. doi:10.1016/j.wasman.2020.02.032

Gardy, J., Hassanpour, A., Lai, X., Ahmed, M. H., and Rehan, M. (2017). Biodiesel Production from Used Cooking Oil Using a Novel Surface Functionalised TiO_2 Nano-Catalyst. *Appl. Catal. B Environ.* 207, 297–310. doi:10.1016/j.apcatb.2017.01.080

Gardy, J., Osatiashtiani, A., Céspedes, O., Hassanpour, A., Lai, X., Lee, A. F., et al. (2018). A Magnetically Separable SO_4/Fe-Al-TiO_2 Solid Acid Catalyst for Biodiesel Production from Waste Cooking Oil. *Appl. Catal. B Environ.* 234, 268–278. doi:10.1016/j.apcatb.2018.04.046

Gardy, J., Rehan, M., Hassanpour, A., Lai, X., and Nizami, A.-S. (2019). Advances in Nano-Catalysts Based Biodiesel Production from Non-food Feedstocks. *J. Environ. Manag.* 249, 109316. doi:10.1016/j.jenvman.2019.109316

Hasan, Z., Yoon, J. W., and Jhung, S. H. (2015). Esterification and Acetylation Reactions over *In Situ* Synthesized Mesoporous Sulfonated Silica. *Chem. Eng. J.* 278, 105–112. doi:10.1016/j.cej.2014.12.025

Hoang, A. T., Tran, V. D., Dong, V. H., and Le, A. T. (2019). An Experimental Analysis on Physical Properties and Spray Characteristics of an Ultrasound-Assisted Emulsion of Ultra-low-sulphur Diesel and Jatropha-Based Biodiesel. *J. Mar. Eng. Technol.* 1-9. doi:10.1080/20464177.2019.1595355

Ingle, A. P., Philippini, R., Martiniano, S. E., da Silva, S. S., and Chandel, A. K. (2020). Application of Metal Oxide Nanostructures as Heterogeneous Catalysts for Biodiesel Production. *Adv. Heterog. CatalystsNano-Scale* Vol. 1, 261–289. *Applications at the*. doi:10.1021/bk-2020-1359.ch009

Joseph, J., Baker, C., Mukkamala, S., Beis, S. H., Wheeler, M. C., DeSisto, W. J., et al. (2010). Chemical Shifts and Lifetimes for Nuclear Magnetic Resonance (NMR) Analysis of Biofuels. *Energy fuels.* 24 (9), 5153–5162. doi:10.1021/ef100504d

Kanakdande, A. P., and Khobragade, C. N. (2020). Biodiesel Synthesis from Non-edible Oil Using Agro-Waste and Evaluation of its Physicochemical Properties. *Int. J. Environ. Sci. Technol.* 17 (8), 3785–3800. doi:10.1007/s13762-020-02731-y

Kaur, N., and Ali, A. (2014). Kinetics and Reusability of Zr/CaO as Heterogeneous Catalyst for the Ethanolysis and Methanolysis of Jatropha Crucas Oil. *Fuel Process. Technol.* 119, 173–184. doi:10.1016/j.fuproc.2013.11.002

Khan, M. B., Kazim, A. H., Farooq, M., Javed, K., Shabbir, A., Zahid, R., et al. (2021). Impact of HHO Gas Enrichment and High Purity Biodiesel on the Performance of a 315 Cc Diesel Engine. *Int. J. Hydrogen Energy* 46 (37), 19633–19644. doi:10.3390/en1322594110.1016/j.ijhydene.2021.03.112

Khan, M. B., Kazim, A. H., Shabbir, A., Farooq, M., Farooq, H., Ali, Q., et al. (2020). Performance and Emission Analysis of High Purity Biodiesel Blends in Diesel Engine. *Adv. Mech. Eng.* 12 (11)

Kostić, M. D., Bazargan, A., Stamenković, O. S., Veljković, V. B., and McKay, G. (2016). Optimization and Kinetics of Sunflower Oil Methanolysis Catalyzed by Calcium Oxide-Based Catalyst Derived from Palm Kernel Shell Biochar. *Fuel* 163, 304–313. doi:10.1016/j.fuel.2015.09.042

Lam, M. K., and Lee, K. T. (2011). Mixed Methanol-Ethanol Technology to Produce Greener Biodiesel from Waste Cooking Oil: A Breakthrough for SO_{42}−/SnO_2-SiO_2 Catalyst. *Fuel Process. Technol.* 92 (8), 1639–1645. doi:10.1016/j.fuproc.2011.04.012

Laskar, I. B., Rokhum, L., Gupta, R., and Chatterjee, S. (2020). Zinc Oxide Supported Silver Nanoparticles as a Heterogeneous Catalyst for Production of Biodiesel from Palm Oil. *Environ. Prog.* 39 (3), e13369. doi:10.1002/ep.13369

Lee, J. H., Jeon, H., Park, J. T., and Kim, J. H. (2020). Synthesis of Hierarchical Flower-Shaped Hollow MgO Microspheres via Ethylene-Glycol-Mediated Process as a Base Heterogeneous Catalyst for Transesterification for Biodiesel Production. *Biomass Bioenergy* 142, 105788. doi:10.1016/j.biombioe.2020.105788

Leung, D. Y. C., Wu, X., and Leung, M. K. H. (2010). A Review on Biodiesel Production Using Catalyzed Transesterification. *Appl. Energy* 87 (4), 1083–1095. doi:10.1016/j.apenergy.2009.10.006

Li, J., Vosegaard, T., and Guo, Z. (2017). Applications of Nuclear Magnetic Resonance in Lipid Analyses: An Emerging Powerful Tool for Lipidomics Studies. *Prog. Lipid Res.* 68, 37–56. doi:10.1016/j.plipres.2017.09.003

Li, K., Liu, C., Jiang, S., and Chen, Y. (2020). Review on Hybrid Geothermal and Solar Power Systems. *J. Clean. Prod.* 250, 119481. doi:10.1016/j.jclepro.2019.119481

Li, M., Chen, J., Huang, Y., Li, M., Lin, X., and Qiu, T. (2020). Reusable and Efficient Heterogeneous Catalysts for Biodiesel Production from Free Fatty Acids and Oils: Self-Solidifying Hybrid Ionic Liquids. *Energy* 211, 118631. doi:10.1016/j.energy.2020.118631

Mahlia, T. M. I., Syazmi, Z. A. H. S., Mofijur, M., Abas, A. E. P., Bilad, M. R., Ong, H. C., et al. (2020). Patent Landscape Review on Biodiesel Production: Technology Updates. *Renew. Sustain. Energy Rev.* 118, 109526. doi:10.1016/j.rser.2019.109526

Mallah, T. A., and Sahito, A. R. (2020). Optimization of castor and Neem Biodiesel Blends and Development of Empirical Models to Predicts its Characteristics. *Fuel* 262, 116341. doi:10.1016/j.fuel.2019.116341

Mumtaz, H., Farhan, M., Amjad, M., Riaz, F., Kazim, A. H., Sultan, M., et al. (2021). Biomass Waste Utilization for Adsorbent Preparation in CO2 Capture and Sustainable Environment Applications. *Sustain. Energy Technol. Assessments* 46, 101288. doi:10.1016/j.seta.2021.101288

Munir, M., Ahmad, M., mubashir, M., Asif, S., Waseem, A., Mukhtar, A., et al. (2021b). A Practical Approach for Synthesis of Biodiesel via Non-edible Seeds Oils Using Trimetallic Based Montmorillonite Nano-Catalyst. *Bioresour. Technol.* 328, 124859. doi:10.1016/j.biortech.2021.124859

Munir, M., Ahmad, M., Rehan, M., Saeed, M., Lam, S. S., Nizami, A. S., et al. (2021a). Production of High Quality Biodiesel from Novel Non-edible Raphnus Raphanistrum L. Seed Oil Using Copper Modified Montmorillonite Clay Catalyst. *Environ. Res.* 193, 110398. doi:10.1016/j.envres.2020.110398

Munir, M., Ahmad, M., Saeed, M., Waseem, A., Nizami, A.-S., Sultana, S., et al. (2021). Biodiesel Production from Novel Non-edible Caper (Capparis Spinosa L.) Seeds Oil Employing Cu-Ni Doped ZrO_2 Catalyst. *Renew. Sustain. Energy Rev.* 138, 110558. doi:10.1016/j.rser.2020.110558

Munir, M., Ahmad, M., Saeed, M., Waseem, A., Rehan, M., Nizami, A.-S., et al. (2019a). Sustainable Production of Bioenergy from Novel Non-edible Seed Oil (Prunus Cerasoides) Using Bimetallic Impregnated Montmorillonite Clay Catalyst. *Renew. Sustain. Energy Rev.* 109, 321–332. doi:10.1016/j.rser.2019.04.029

Munir, M., Saeed, M., Ahmad, M., Waseem, A., Sultana, S., Zafar, M., et al. (2019b). Optimization of Novel Lepidium Perfoliatum Linn. Biodiesel Using Zirconium-Modified Montmorillonite Clay Catalyst. *Energ Source Part*, 1. doi:10.1080/15567036.2019.1691289

Musa, I. A. (2016). The Effects of Alcohol to Oil Molar Ratios and the Type of Alcohol on Biodiesel Production Using Transesterification Process. *Egypt. J. Petroleum* 25 (1), 21–31. doi:10.1016/j.ejpe.2015.06.007

Mustapha, S., Ndamitso, M. M., Abdulkareem, A. S., Tijani, J. O., Shuaib, D. T., Mohammed, A. K., et al. (2019). Comparative Study of Crystallite Size Using Williamson-Hall and Debye-Scherrer Plots for ZnO Nanoparticles. *Adv. Nat. Sci. Nanosci. Nanotechnol.* 10 (4), 045013. doi:10.1088/2043-6254/ab52f7

Napolitano, M., Terzaroli, N., Kashyap, S., Russi, L., Jones-Evans, E., and Albertini, E. (2020). Exploring Heterosis in Melon (Cucumis Melo L.). *Plants* 9 (2), 282. doi:10.3390/plants9020282

Nesom, G. (2011). New State Records for Citrullus, Cucumis, and Cucurbita (Cucurbitaceae) outside of Cultivation in the USA. *Phytoneuron* 1, 1

Nuñez-Palenius, H. G., Ramírez-Malagón, R., and Ochoa-Alejo, N. (2011). Muskmelon Embryo Rescue Techniques Using *In Vitro* Embryo Culture. *Plant Embryo Cult.* 710, 107–115. doi:10.1007/978-1-61737-988-8_9

Okwundu, O. S., El-Shazly, A. H., and Elkady, M. (2019). Comparative Effect of Reaction Time on Biodiesel Production from Low Free Fatty Acid Beef Tallow: a Definition of Product Yield. *SN Appl. Sci.* 1 (2), 140. doi:10.1007/s42452-018-0145-1

Oueda, N., Bonzi-Coulibaly, Y. L., and Ouédraogo, I. W. K. (2017). Deactivation Processes, Regeneration Conditions and Reusability Performance of CaO or MgO Based Catalysts Used for Biodiesel Production-A Review. *Msa* 08 (01), 94–122. doi:10.4236/msa.2017.81007

Pasae, Y., Tangdilintin, S., Bulo, L., and Allo, E. L. (2020). The Contribution of Heterogeneous and Homogeneous Catalysts towards Biodiesel Quality. *J. Phys. Conf. Ser.*, 1464. 012054. doi:10.1088/1742-6596/1464/1/012054

Petkova, Z., and Antova, G. (2015). Proximate Composition of Seeds and Seed Oils from Melon (Cucumis Melo L.) Cultivated in Bulgaria. *Cogent Food & Agric.* 1 (1), 1018779. doi:10.1080/23311932.2015.1018779

Rahman, F. A., Aziz, M. M. A., Saidur, R., Bakar, W. A. W. A., Hainin, M. R., Putrajaya, R., et al. (2017). Pollution to Solution: Capture and Sequestration of Carbon Dioxide (CO_2) and its Utilization as a Renewable Energy Source for a Sustainable Future. *Renew. Sustain. Energy Rev.* 71, 112–126. doi:10.1016/j.rser.2017.01.011

Rashid, U., Soltani, S., Al-Resayes, S. I., and Nehdi, I. A. (2018). *Metal Oxides in Energy Technologies*. Elsevier, 303–319. doi:10.1016/B978-0-12-811167-3.00011-0

Rasouli, H., and Esmaeili, H. (2019). Characterization of MgO Nanocatalyst to Produce Biodiesel from Goat Fat Using Transesterification Process. *3 Biotech.* 9 (11), 429–511. doi:10.1007/s13205-019-1963-6

Razavi, R., Bemani, A., Baghban, A., Mohammadi, A. H., and Habibzadeh, S. (2019). An Insight into the Estimation of Fatty Acid Methyl Ester Based Biodiesel Properties Using a LSSVM Model. *Fuel* 243, 133–141. doi:10.1016/j.fuel.2019.01.077

Razzaq, L., Farooq, M., Mujtaba, M. A., Sher, F., Farhan, M., Hassan, M. T., et al. (2020). Modeling Viscosity and Density of Ethanol-Diesel-Biodiesel Ternary Blends for Sustainable Environment. *Sustainability* 12 (12), 5186. doi:10.3390/su12125186

Razzaq, L., Imran, S., Anwar, Z., Farooq, M., Abbas, M. M., Mehmood Khan, H., et al. (2020). Maximising Yield and Engine Efficiency Using Optimised Waste Cooking Oil Biodiesel. *Energies* 13 (22), 5941. doi:10.3390/en13225941

Rehan, M., Gardy, J., Demirbas, A., Rashid, U., Budzianowski, W. M., Pant, D., et al. (2018). Waste to Biodiesel: A Preliminary Assessment for Saudi Arabia. *Bioresour. Technol.* 250, 17–25. doi:10.1016/j.biortech.2017.11.024

Rizwanul Fattah, I. M., Ong, H. C., Mahlia, T. M. I., Mofijur, M., Silitonga, A. S., Rahman, S. M. A., et al. (2020). State of the Art of Catalysts for Biodiesel Production. *Front. Energy Res.* 8, 101. doi:10.3389/fenrg.2020.00101

Rozina, M., Ahmad, M., Zafar, M., and Ali, N. (2019). Biodiesel Synthesis and Physiochemical Analysis of *Taraxacum officinale* F.H.Wigg Seed Oil. *Int. J. Environ. Sci. Technol.* 16 (8), 4103–4112. doi:10.1007/s13762-019-02336-0

Saeed, M. A., Farooq, M., Anwar, A., Abbas, M. M., Soudagar, M. E. M., Siddiqui, F. A., et al. (2021). Flame Propagation and Burning Characteristics of Pulverized Biomass for Sustainable Biofuel. *Biomass Conv. bioref.* 11 (2), 409–417. doi:10.1007/s13399-020-00875-y

Sahithi, G., Vasanthi, R., Banji, D., Rao, K., and Selvakumar, D. (2015). Study of Phytochemical and Antioxidant Activity of Cucumis Melo Var. Agrestis Fruit. *J. Pharmacogn. Phytochem.* 4 (2), 63. doi:10.1016/j.biortech.2007.11.063

Saydut, A., Duz, M., Kaya, C., Kafadar, A., and Hamamci, C. (2008). Transesterified Sesame (Sesamum indicum L.) Seed Oil as a Biodiesel Fuel. *Bioresour. Technol.* 99 (14), 6656–6660. doi:10.1016/j.biortech.2007.11.063

Shaheen, A., Sultana, S., Lu, H., Ahmad, M., Asma, M., and Mahmood, T. (2018). Assessing the Potential of Different Nano-Composite (MgO, Al_2O_3 -CaO and TiO_2) for Efficient Conversion of Silybum Eburneum Seed Oil to Liquid Biodiesel. *J. Mol. Liq.* 249, 511–521. doi:10.1016/j.molliq.2017.11.053

Shahzad, K., Nizami, A. S., Sagir, M., Rehan, M., Maier, S., Khan, M. Z., et al. (2017). Biodiesel Production Potential from Fat Fraction of Municipal Waste in Makkah. *PloS one* 12 (2), e0171297. doi:10.1371/journal.pone.0171297

Sharma, A., Singh, Y., Kumar Singh, N., Singla, A., Chyuan Ong, H., and Chen, W.-H. (2020). Effective Utilization of Tobacco (Nicotiana Tabaccum) for Biodiesel Production and its Application on Diesel Engine Using Response Surface Methodology Approach. *Fuel* 273, 117793. doi:10.1016/j.fuel.2020.117793

Silva, M. A., Albuquerque, T. G., Alves, R. C., Oliveira, M. B. P. P., and Costa, H. S. (2020). Melon (Cucumis Melo L.) By-Products: Potential Food Ingredients for Novel Functional Foods? *Trends Food Sci. Technol.* 98, 181–189. doi:10.1016/j.tifs.2018.07.005

Tamilselvi, P., Yelilarasi, A., Hema, M., and Anbarasan, R. (2013). Synthesis of Hierarchical Structured MgO by Sol-Gel Method. *Nano Bull.* 2 (1), 130106.

Teo, S. H., Rashid, U., and Taufiq-Yap, Y. H. (2014). Green Nano-Catalyst for Methanolysis of Non-edible Jatropha Oil. *Energy Convers. Manag.* 87, 618–627. doi:10.1016/j.enconman.2014.07.048

Thangaraj, B., Solomon, P. R., Muniyandi, B., Ranganathan, S., and Lin, L. (2019). Catalysis in Biodiesel Production-A Review. *Clean. Energy* 3 (1), 2–23. doi:10.1093/ce/zky020

Ullah, K., Jan, H. A., Ahmad, M., and Ullah, A. (2020). Synthesis and Structural Characterization of Biofuel from Cocklebur sp., Using Zinc Oxide Nano-Particle: A Novel Energy Crop for Bioenergy Industry. *Front. Bioeng. Biotechnol.* 8, 756. doi:10.3389/fbioe.2020.00756

Ullah, K., Sharma, V. K., Ahmad, M., Lv, P., Krahl, J., Wang, Z., et al. (2018). The Insight Views of Advanced Technologies and its Application in Bio-Origin Fuel Synthesis from Lignocellulose Biomasses Waste, a Review. *Renew. Sustain. Energy Rev.* 82, 3992–4008. doi:10.1016/j.rser.2017.10.074

Verziu, M., Cojocaru, B., Hu, J., Richards, R., Ciuculescu, C., Filip, P., et al. (2008). Sunflower and Rapeseed Oil Transesterification to Biodiesel over Different Nanocrystalline MgO Catalysts. *Green Chem.* 10 (4), 373–381. doi:10.1039/b712102d

Wang, D., Jiang, D., Fu, J., Hao, M., and Peng, T. (2021). Assessment of Liquid Biofuel Potential from Energy Crops within the Sustainable Water–Land–Energy–Carbon Nexus. *Sustain. Energy Fuels.* 75, 814. doi:10.1039/D0SE00814A

Yang, S-C., Chang, J-R., Lee, M-T., Lin, T-b., Lee, F-M., Hong, C-t., et al. (2014). *Homogeneous Catalysts for Biodiesel Production*. Google Patents.

Yusuff, A. S., Gbadamosi, A. O., and Popoola, L. T. (2021). Biodiesel Production from Transesterified Waste Cooking Oil by Zinc-Modified Anthill Catalyst: Parametric Optimization and Biodiesel Properties Improvement. *J. Environ. Chem. Eng.* 9, 104955. doi:10.1016/j.jece.2020.104955

Conflict of Interest: The authors declare that the research was conducted in the absence of any commercial or financial relationships that could be construed as a potential conflict of interest.

Publisher's Note: All claims expressed in this article are solely those of the authors and do not necessarily represent those of their affiliated organizations, or those of the publisher, the editors, and the reviewers. Any product that may be evaluated in this article, or claim that may be made by its manufacturer, is not guaranteed or endorsed by the publisher.